Advances in Geosciences 地球科学前沿, 2021, 11(1), 60-93
Published Online January 2021 in Hans. http://www.hanspub.org/journal/ag
https://doi.org/10.12677/ag.2021.111006

闪锌矿中稀散元素镓和铟的富集规律研究

张学义[1]**，孙文燕**[2*]

[1]中国冶金地质总局，北京
[2]中国地质科学院，北京
Email: zhangxueyi_252@126.com, *swy_hx@163.com

收稿日期：2020年12月21日；录用日期：2021年1月21日；发布日期：2021年1月28日

摘　要

闪锌矿是镓(Ga)和铟(In)最重要的载体矿物，它在各种类型的矿床中普遍存在。Ga和In已被美国、欧盟、英国、中国等列入关键矿产名录，其在战略新兴产业发展中有非常重要的作用，是平板显示屏、电子半导体和光伏电池等产业必不可少的原料。在本研究中，运用ICPMS技术对澳大利亚和其他国家各类矿床闪锌矿样品中微量元素的含量进行了分析。所得出的结果与相关文献中收集的数据结合在一起，分析Ga和In在不同类型矿床中的分布情况(矿床类型包括矿床工业类型与矿床成因类型)。研究发现，Ga主要分布在热液矿床、层控矿床及银(Ag)矿床中；而In通常在热液矿床、喷流–沉积矿床(SEDEX)和锡(Sn)矿床中含量较高。同时也探讨了Ga和In之间的关系，Ga/In的比率可以用于区别矿床成因类型，即在层控矿床和密西西比河谷型(MVT)矿床中Ga/In > 1；在网状脉矿床中Ga/In ≈ 1；在热液、矽卡岩、火山成因块状硫化物(VMS)和SEDEX矿床中Ga/In < 1。Ga和In的富集均与Cu相关，且Ga的富集与Ag相关，因此分别为下列置换提供了证据：$(Ag, Cu)^+ + Ga^{3+} \leftrightarrow 2Zn^{2+}$和$Cu^+ + In^{3+} \leftrightarrow 2Zn^{2+}$。Ga与Co含量的负相关性表明富含Co的闪锌矿相对贫Ga，但是对于这一现象还没有明确的解释。

关键词

闪锌矿，镓，铟，矿床类型，关键矿产

Trace and Minor Elements in Sphalerite: A Study of Gallium and Indium

Xueyi Zhang[1]**, Wenyan Sun**[2*]

[1]China Metallurgical Geology Bureau, Beijing
[2]Chinese Academy of Geological Sciences, Beijing
Email: zhangxueyi_252@126.com, *swy_hx@163.com

Received: Dec. 21st, 2020; accepted: Jan. 21st, 2021; published: Jan. 28th, 2021

*通讯作者。

文章引用: 张学义, 孙文燕. 闪锌矿中稀散元素镓和铟的富集规律研究[J]. 地球科学前沿, 2021, 11(1): 60-93.
DOI: 10.12677/ag.2021.111006

Abstract

Sphalerite is the most important host mineral of gallium (Ga) and indium (In) as it is commonly observed in a wide range of deposit types. Ga and In have been listed as critical minerals by the United States, the European Union, the United Kingdom, China and other countries. Ga and In play a very important role in the development of strategic emerging industries, and are essential raw materials for industries, such as flat screens, electronic semiconductors and photovoltaic cells. In this study, ICPMS techniques have been used to investigate the distribution of minor and trace elements in sphalerite samples from both Australian and international deposits. These new results have been combined with data available in the literature, to examine the distributions of Ga and In in different types of deposits (both industrial types and genetic types). Gallium is found to be concentrated in hydrothermal, stratabound and Ag deposits, while indium is usually highest in sphalerite from hydrothermal, SEDEX and Sn deposits. The relationship between Ga and In is also explored, and the ratio of Ga/In can broadly discriminate between the genetic types. That is, in stratabound and MVT deposits Ga/In > 1; in stockwork deposits Ga/In ≈ 1; in hydrothermal, skarn, VMS and SEDEX deposits Ga/In < 1. Both gallium and indium concentrations correlate with Cu, and gallium concentration correlates with Ag, providing supporting evidence for the coupled $(Ag, Cu)^{+} + Ga^{3+} \leftrightarrow 2Zn^{2+}$ and $Cu^{+} + In^{3+} \leftrightarrow 2Zn^{2+}$ substitutions respectively. The negative correlation between Ga and Co indicates that Co-rich sphalerite has relatively low Ga concentration, but an explanation for this remains unclear.

Keywords

Sphalerite, Gallium, Indium, Deposit Type, Critical Minerals

1. 引言

闪锌矿是世界上非常重要的锌矿石矿物，且在所有富硫化物的碱金属矿床中都有出现[1]。闪锌矿的晶体结构可以容纳多种微量元素，因而非常适合微量元素研究[2]。在许多锌矿床中，闪锌矿不仅是 Zn 的主要来源，还是 Cd，Ga，Ge 和 In 等元素的主要载体[3]-[8]。Gatterer (1941)对闪锌矿的形成温度与微量元素含量之间的关系进行了研究，显示 Co 和 In 富集在超高温热液矿床中，而 Ga 和 Ge (Hg、Sn)则富集于低温矿床中，在低温组合中，富 Ga 闪锌矿的形成温度高于富 Ge 闪锌矿的形成温度[9]。Cook 等(2009)研究了不同类型矿床中元素的特征，并指出闪锌矿中微量元素的组成或许可以用来指示矿床成因，但是研究中并没有给出分析矿床成因的具体方法[10]。

前文已提及闪锌矿是稀散元素 Ga 和 In 的主要载体，而 Ga 和 In 已被美国、欧盟、英国、中国等列入关键矿产名录，中国则是 Ga 和 In 的最大生产国[11]。赵汀等(2017)对镓矿资源的需求趋势进行了分析，预测出全球 2020 年镓金属需求约 410~430 吨[12]。毛景文等(2019b)针对关键金属矿床的成矿作用与成矿环境，同时考虑共伴生特点，将主要的关键矿床分为 8 种成因类型，其中 Ga、In 属于多种类型热液矿床中的伴生组分[13]。陈伟波等(2019)对铟矿资源的供需现状进行了分析，认为未来我国将可能成为铟纯进口国[14]。郭妍冉等(2019)对镓矿资源分布、生产现状及消费特点进行了分析研究[15]。徐净和李晓峰

(2018)、李晓峰等(2019)对铟的主要矿床类型进行了总结，并预测未来 SEDEX 和 VMS 矿床有可能成为铟资源的主要来源，而火山岩中铟的异常富集也应引起重视[16] [17]。Ga 和 In 在战略新兴产业发展中有非常重要的作用，是平板显示屏、电子半导体和光伏电池等产业必不可少的原料。鉴于 Ga 和 In 的重要程度，以及其与闪锌矿的密切关系，研究闪锌矿中 Ga 和 In 的富集规律对于寻找 Ga 和 In 具有十分重要的意义。

本文采用 ICPMS 溶液分析法获得 38 件闪锌矿样品中微量元素的含量。所得结果与在文献中收集的数据相结合，通过分析 Ga 和 In 在不同类型矿床中的含量变化，以及 Ga 和 In 之间，Ga 或 In 与其他微量元素(如 Cu、Sn、Ag、Co、Zn 等)之间的相关性，来推测哪些类型矿床中的闪锌矿富含 Ga 或 In。

2. 样品概况

本文分析的样品主要来自澳大利亚，少量来自世界其他地方的矿床，由维多利亚博物馆提供。样品来自不同类型的矿床，详细信息见表 1。表 1 中的所有标本均在澳大利亚墨尔本大学地球科学学院分析测试，样品 1~18 全部来自澳大利亚的矿床，第一批进行的测试分析；其他 20 件样品来自澳大利亚及世界其他地方的矿床，第二批进行的测试分析。从文献中收集的样品数据见附表 1。

本次研究的样品所属矿床的成因依据其成矿背景进行分类，包括网脉状(Stockwork)、矽卡岩型(Skarn)、层控型(Stratabound)、海相火山成因块状硫化物(VMS)、喷流－沉积型(SEDEX)和密西西比河谷型(MVT)矿床，其中仅一件样品来自造山型(Orogenic)矿床。若无法获得足够的信息，则以矿石形成过程分类，如热液(Hydrothermal)矿床。花岗－伟晶岩型(Granite-pegmatite hosted，表 1，样品 17~22)和砂岩型(Sandstone-hosted，附表 1，样品 100~103)矿床样品的分类由博物馆馆长及相关文献提供。具体成因类型不明确时，如无法判断是层控型、矽卡岩型或 MVT 型，将使用后生成因分类(Epigenetic，表 1，样品 6~8)。样品的矿床工业类型基本清楚，但在分析过程中，Zn-Pb-Ag 和 Pb-Zn-Ag，Zn-Pb-Cu 和 Cu-Zn-Pb，Pb-Zn/Zn-Pb 和 Zn，Ag 和 Ag-Au，Cu 和 Cu-Au 因其相似性归为一类。

Table 1. Detailed information of samples analyzed in this study
表 1. 本文所分析样品详细信息

序号	样品编号	采样位置	成因类型	工业类型	开采历史；储量，品位	参考文献
1	M9306	Australia, Queensland, John Bull No.1 South, 3 miles south of Ravenswood	Stockwork	Au	1978~now; 4 Moz @ 1.6 g/t	[18] [19]
2	M9317	Australia, Tasmania, Mount Bischoff Tin Mining Company	Skarn	Sn	1871~1947, restarted in 2008; 62,000 t of metallic tin	[20]
3	M9321	Australia, South Australia, Talisker mine, 11 km east of Cape Jervis (35˚36'S, 138˚8'E)	VMS	Ag-Pb	1862~1935; 4.5 t Ag	[21]
4	M9323	Australia, Western Australia, Murchison Division, Northampton district, Wheal Ellen	Stratabound	Zn-Pb-Ag	1880's~now	[22] [23] [24]
5	M14937	Australia, Victoria, Maldon, South German mine, 470 foot level (37˚0'S, 144˚4'E)	Orogenic	Au	1857~1926	[25] [26] [27]
6	M18746	Australia, Victoria, Mount Deddick (37˚6'S, 148˚28'E)	*Epigenetic*	Ag-Pb	1896~unknown; 20 tons of Pb	[28]
7	M24424	Australia, Tasmania, Rosebery, Rosebery mine (41˚47'S, 145˚34'E)	VMS	Zn-Pb-Cu	1936~now; 20 Mt ore	[29] [30] [31] [32]

Continued

8	M24431	Australia, Tasmania, Dundas, South Comet mine (41˚53'S, 145˚25'E)	*Epigenetic*	Ag-Pb	Old, reopened in the mid 1980's to unknown	[33]
9	M25640	Australia, South Australia, Kadina, Wallaroo mines (33˚58'S, 137˚43'E)	—	Cu	—	[34]
10	M37225	Australia, Western Australia, Agnew Nickel Deposit, near Kambalda	Stockwork	Ni	45 million metric tons at 2.05% Ni	[35] [36] [37]
11	M38825	Australia, Tasmania, Hellyer mine, 90 km south-south-west of Burnie (41˚36'S, 145˚42'E)	VMS	Zn-Pb-Cu	16.2 million metric tons ore	[29] [30] [38]
12	M41383	Australia, New South Wales, Red Rock, near Drake	Stockwork	Ag-Au	1886~unknown; 180,000 t of 67 g/t Ag and 0.9 g/t Au (reported 1984)	[39] [40]
13	M50203	Australia, New South Wales, Broken Hill, South mine, No. 7 shaft, 1630 foot level, G21, 90 feet above level (31˚58'S, 141˚27'E)	Stratabound	Pb-Zn-Ag	—	[41]
14	M50249	Australia, New South Wales, Broken Hill, Section 32 (stope), 16 level, Zinc Corporation (31˚58'S, 141˚27'E)	Stratabound	Pb-Zn-Ag	—	[42]
15	M50250	Australia, Tasmania, Zeehan, Comstock lode, Swansea mine (41˚53'S, 145˚20'E)	Stratabound	Ag-Pb	—	[43]
16	M50251	Australia, Queensland, Bloomsbury, Mixer (Godkin) mine (20˚42'S, 148˚35'E)	—	—	—	—
17	M50256	Australia, New South Wales, New England District, Emmaville, Webbs Consols mine (29˚26'S, 151˚36'E)	*Granite-pegmatite hosted*	Pb-Zn-Ag	1884~1970's; ~19,000 t of ore	[44] [45]
18	M50345	Australia, Victoria, Lilydale, Cave Hill	MVT	Pb-Zn	—	—
19	M2064	New Zealand, South Island, Tasman, Collingwood, 80 km north-west of Nelson	—	—	—	—
20	M4983	Spain, Picos de Europa	MVT	Pb-Zn	1860~1990	[46] [47]
21	M9318	Australia, Tasmania, Mount Zeehan, Silver Bell mine	Skarn	—	—	[48]
22	M11785	Australia, New South Wales, New England District, Emmaville, Webbs Consols mine	*Granite-pegmatite hosted*	Pb-Zn-Ag	1884~1970's; ~19,000 t of ore	[44] [45]
23	M22706	Australia, New South Wales, Leadville	Skarn	Zn-Pb	Late 1890's	[49] [50]
24	M22716	New Zealand, South Island, Nelson	—	Cu	—	[51]
25	M25639	Wales UK, Wrexham (Denbighshire; Clwyd), Minera, Minera mines	—	Pb-Zn	—	[52]
26	M28838	United States of America, Kansas, Cherokee County, Baxter Springs	—	—	—	—
27	M29038	United States of America, Kansas, Cherokee County, Treece	MVT	Pb-Zn	—	—

Continued

28	M35909A	Kosovo (formerly Serbia), Trepca Complex, Stari Trg mine, 8 km east of Kosovska Mitrovica (42˚52'S, 20˚52'E)	Hydrothermal	Pb-Zn-Ag	Late 1950's-1998/99, reopened in 2005	[53] [54] [55]
29	M35909B					
30	M39582A	Greenland, Kvanefjeld, dumps, 5 km north-north-west of Narsaq	Stockwork	U-Th-REE	1978~1984	[56] [57]
31	M39582B					
32	M42805	Japan, No 5 Orebody, Mozumi deposit, Kamioka Mine, Yoshiki-gun, Hida Dist. Gifu Pref.	Skarn	Pb-Zn-Ag	—	[58]
33	M45431	England, Cornwall, Bissoe, Wheal Jane, 4 km north-east of Gwennap	Hydrothermal	Sn	1740~1991; 4,747.5 tons of black tin, 580,339 tons of tin ore at ~0.6%	[59] [60] [61]
34	M45751	Kosovo (formerly Serbia), Trepca Complex, Stari Trg mine, 8 km east of Kosovska Mitrovica (42˚52'S, 20˚52'E)	Hydrothermal	Pb-Zn-Ag	Late 1950's~1998/99, reopened in 2005	[53] [54] [55]
35	M46386	Canada, Northwest Territories, Baffin Island, Nanisivik mine (72˚N, 85˚W)	MVT	Pb-Zn-Ag	1976~2002; 6.5 million metric tons of 12% Zn, 1.5% Pb and 50 g/t Ag	[62]-[67]
36	M46387	Ireland, County Tipperary, Silvermines	Stratabound	Zn-Pb	1968~1982 exploited by Mogul of Ireland Ltd.; 160 Mt of 7.2% Zn and Pb	[68]-[73]
37	M48600	Australia, Western Australia, Goongewa mine, near Fitzroy Crossing	MVT	Zn-Pb	—	[74] [75]
38	M50202	Australia, New South Wales, Broken Hill, Zinc Corporation mine, 16 level, footwall of No.2 lens (31˚58'S, 141˚27'E)	Stratabound	Pb-Zn-Ag	—	[42]

3. 分析方法

为得到各种成矿环境中闪锌矿微量元素的含量，采用 ICPMS 溶液分析法分析了 38 件样品。在稀释之前，这些样品经过碎样，精心挑选和研磨，准备进行分析，ICPMS 溶液分析法实验流程如下：

将所有的聚四氟乙烯实验器皿按顺序进行清洗。将约 5 mg 闪锌矿粉末溶于 2 ml 16 N HNO_3 中，将装有闪锌矿粉末溶液的 PFA 烧杯放在 130℃的热板上一整晚。然后再将样品放在用酸清洗过的 12 ml 聚碳酸酯离心管中，用 18.2 摩尔水稀释。所得溶液用包含一种内部标准混合物的 1.3% HNO_3 进一步稀释，总稀释系数约为 60,000。分析和漂移校正的过程如 Eggins *et al.* (1997)所述[76]。该方法使用天然岩石标准进行校正，内部漂移使用内部标准(Li_6, Ni_{61}, Sr_{84}, Rh, Sm_{147}, Re, and U_{235})、外部漂移监测和积极的冲刷多方面结合进行校正。与 Eggins *et al.* (1997)的方法的不同之处是：1) Tm，In 和 Bi 没有使用内部标准。2) USGS 标准 W-2 被用作校正标准。W-2 的首选浓度主要是通过对合成标准的分析和同位素稀释分析的文献调查得出的。3) W-2 的溶解加入了额外的 Zn、Ag、Cd、In 和 Pb，以便使这些元素的浓度与预期的闪锌矿类似。

本文样品在墨尔本大学地球科学学院 Agilent 7700x ICPMS 仪器上进行分析，其中氧化铈低于 0.9%。每一同位素重复 4 次实验，每次 100 次扫描。停顿时间是 10 毫秒。

样品的冲洗时间长达 6 分钟，使用的溶液为 5% HNO_3 与 0.5% Triton X-100 和 0.025% HF。样品吸收时间长达 100 秒，使用 5% HNO_3 和 2% HNO_3 溶液。每测试 6 到 8 个样品即对漂移监测器进行一次分析。

Table 2. Concentrations for minor and trace elements in sphalerite samples of Table 1 (ppm, except Fe)
表 2. 表 1 中闪锌矿样品主微量元素含量(ppm，Fe 除外)

样品编号	Ti	Fe (%)	Co	Ni	Cu	Zn	Ga	As	Nb	Mo	Ag	Cd	In	Sn	Sb	Tl	Pb	Bi
Unknown deposits																		
M25640	3.80	1.82	319.12	0.97	121.80	625,559.3	0.05	0.15	0.003	0.01	1.02	985.8782	190.97	2.92	0.29	0.001	16.74	0.000
M50251	4.78	0.18	29.53	0.43	49.88	634,378.6	0.15	0.13	0.002	0.01	1.58	2550.154	74.20	0.31	0.14	0.001	3.11	0.000
M2064	29.95	0.00	0.17	0.10	21.60	627,607	3.88	4.62	0.000	0.02	0.70	5072.475	6.83	0.47	0.93	0.002	22.75	0.097
M22716	29.09	0.00	1.46	1.95	25.11	623,556.7	1.60	12.74	0.006	0.23	3.60	5032.235	4.87	0.44	3.65	0.002	169.91	0.523
M25639	32.28	0.00	7.33	—	3623.00	568,268.3	9.75	2.07	0.002	0.01	94.84	5123.457	0.01	0.04	139.90	0.246	136.38	0.009
M28838	33.59	0.00	4.36	2.59	1116.47	637,162	450.64	0.39	0.011	0.47	0.43	3029.735	1.58	0.80	3.50	0.258	41.43	1.505
Epigenetic deposits																		
M18746	3.11	5.64	10.30	1.24	1709.38	582,956.2	11.11	9.30	0.001	0.02	8.68	2334.555	1.37	1768.06	3.82	0.004	29.43	0.000
M24431	4.17	4.00	34.57	5.80	399.93	584,979.2	0.67	164.61	0.002	0.02	136.45	2372.329	2.39	3.85	172.59	0.021	1310.36	0.000
Granite-pegmatite hosted deposits																		
M50256	3.17	8.58	2.40	0.20	3458.64	365,676.2	2.15	29.88	0.017	0.09	3352.69	1636.269	114.20	34.46	74.81	1.011	227,066.36	0.000
M11785	30.28	0.00	0.50	5.84	725.08	513,548.1	6.01	4.73	0.019	0.16	17.84	3215.146	257.57	3.55	1.42	0.018	59.98	0.181
Hydrothermal deposits																		
M35909A	31.79	0.00	142.65	2.77	283.02	636,810.8	0.83	0.59	—	0.00	2.20	3895.022	2.67	0.51	0.95	0.020	7.49	0.018
M35909B	27.98	0.00	119.18	2.45	587.67	542,474.1	0.78	0.80	0.004	0.01	1.63	3310.571	2.15	3.25	3.12	0.037	7.68	0.087
M45431	27.27	0.00	5.62	1.12	1527.13	530,711.4	1.97	1328.94	0.002	0.03	18.83	1354.885	66.61	1133.49	12.75	0.011	387.32	2.264
M45751	28.78	0.00	0.15	—	509.01	560,787.5	2.51	0.17	0.047	0.04	0.83	2539.082	5.51	267.20	3.80	0.003	29.60	0.643
MVT deposits																		
M50345	4.38	2.42	3.64	3.86	246.42	615,412.7	40.36	0.79	0.003	0.02	10.34	3427.963	0.15	134.28	1.50	0.002	2128.67	0.000
M4983	25.70	0.00	12.17	—	47.98	650,347.4	33.22	0.07	0.002	0.01	0.13	904.1849	0.20	3.77	0.16	0.001	4.68	0.106
M46386	25.43	0.00	76.80	0.09	53.09	623,250.7	95.54	0.31	0.002	0.01	88.80	3564.878	55.34	3.55	0.52	0.050	351.65	0.038
M48600	42.62	0.00	1.21	3.34	720.78	613,164.4	44.21	14.10	0.010	0.14	90.25	2312.12	0.56	0.32	136.79	5.879	2114.06	0.129

Continued

样品编号	Ti	Fe (%)	Co	Ni	Cu	Zn	Ga	As	Nb	Mo	Ag	Cd	In	Sn	Sb	Tl	Pb	Bi
M29038	33.28	0.00	3.95	0.79	395.31	638,222.6	48.41	1.24	0.053	0.03	0.10	4244.542	0.02	0.16	0.52	0.022	10.98	0.046
Orogenic deposits																		
M14937	2.14	14.92	3.11	2.09	6301.34	448,603.5	4.33	1.93	0.004	0.06	1.34	10,911.59	288.90	9.38	6.09	0.017	70.08	0.000
Skarn deposits																		
M9317	2.96	10.60	1.82	0.53	8781.88	426,104.6	284.44	3.82	0.002	0.04	141.91	1892.047	1378.79	7464.12	20,139.48	0.039	59,082.82	0.000
M9318	32.41	0.00	8.47	2.33	184.73	632,147.6	8.30	1.93	0.015	0.09	70.43	6662.762	30.60	4.59	119.59	0.023	1716.59	0.804
M22706	25.65	0.00	1.66	—	321.52	535,355.7	3.38	1.67	0.001	0.01	9.70	3270.544	223.25	2.58	0.23	0.002	3.93	0.110
M42805	28.50	0.00	248.43	1.06	16.55	580,439.7	0.33	0.29	0.007	0.05	35.02	3881.986	12.84	7.34	0.46	0.166	1479.02	748.010
Stockwork deposits																		
M9306	3.34	3.10	19.25	3.02	1367.28	458,772.7	2.36	576.18	0.001	0.18	301.69	1874.664	0.83	117.46	62.16	0.140	47,449.05	0.000
M37225	3.46	8.55	935.13	8.74	76.50	556,008.5	17.63	0.81	0.006	0.07	2.83	931.1024	36.63	0.50	0.06	0.005	5.39	0.000
M41383	4.87	0.79	70.85	0.82	839.82	597,627.7	6.97	7.07	0.004	1.47	16.22	3307.291	1.39	3.06	0.27	0.004	802.61	0.000
M39582A	27.14	0.00	2.74	—	9.63	621,775.3	0.36	0.05	18.791	0.02	0.94	23.37542	0.63	1.02	0.26	0.050	13.31	0.055
M39582B	40.15	0.00	2.44	—	9.20	634,809	0.18	0.07	3.645	0.03	0.46	11.67669	0.14	0.72	0.12	0.081	7.11	0.101
Stratabound deposits																		
M9323	3.50	0.96	233.84	0.57	395.37	625,054.8	496.58	0.24	0.001	0.02	3.96	1639.922	28.84	1.25	0.68	0.006	350.01	0.000
M50203	2.10	9.69	260.32	1.73	277.29	527,824.4	2.13	0.10	0.001	0.03	4.02	1078.781	3.34	0.86	2.56	0.006	333.27	0.000
M50249	9.99	11.11	369.68	4.40	8586.00	491,709.8	13.87	1.33	0.029	38.22	10.05	1142.573	4.07	19.47	25.97	0.017	8135.73	0.000
M50250	7.79	0.75	8.21	1.08	77.81	621,073.3	1.88	5.16	0.008	0.02	9.42	2388.721	0.86	12.91	19.59	0.020	512.00	0.000
M46387	27.41	0.00	0.49	0.63	207.57	642,710.9	118.61	5.43	0.010	0.10	0.60	3745.006	17.93	85.74	3.17	0.647	104.29	0.046
M50202	30.48	0.00	83.41	0.50	4850.53	482,586.2	5.20	0.05	0.001	0.00	156.38	1611.557	3.72	8.48	56.79	0.117	72,216.57	2.636
VMS deposits																		
M9321	2.85	8.28	0.97	1.79	83.17	460,123.9	0.25	29.62	0.002	0.15	353.48	2523.473	82.49	6.34	133.13	0.242	119,154.65	0.000
M24424	2.99	6.51	0.64	0.28	184.12	582,064.7	2.31	0.67	0.003	0.01	9.60	703.5986	5.60	0.10	14.30	0.055	104.72	0.000
M38825	4.04	4.64	4.68	0.39	1665.23	573,895.9	1.14	93.29	0.001	0.19	2.33	1096.564	93.27	2.83	4.34	0.140	218.05	0.000

Table 3. Concentrations for minor and trace elements in sphalerite samples of attached Table 1 (samples No. 1~40 of attached Table 1, ppm, except Fe)

表 3. 附表 1 闪锌矿样品主微量元素含量(附表 1 序号 1~40 的样品，ppm，Fe 除外)

样品编号	Mn	Fe (%)	Co	Ni	Cu	Ga	As	Mo	Ag	Cd	In	Sn	Sb	Tl	Pb	Bi	Ge	Se
Hydrothermal deposits																		
Baia de Aries BdA (6)	8040	4.38	—	0.1	1353	3.2	—	0.2	3	4653	141	4	0.1	0.3	0.7	0.2	0.9	4.5
Hanes H-1962 (8)	4532	8.96	8	—	719	3	—	—	12	4052	46	54	1	—	7	7	1	11
Larga L-82 (8)	874	10.44	100	—	1088	5	—	—	9	5560	669	333	—	—	1	—	1	248
Rosia Montana CRC-7 (10)	44,516	1.27	—	—	754	366	—	3	8	2707	38	47	3	—	6	—	73	9
Rosia Montana RM-21 (10)	67,573	0.34	1	—	1906	95	—	2	7	3502	9	17	1	—	343	—	6	8
Magura Mag-8 (8)a	24,400	0.06	—	—	1261	61	223	1	102	4463	1	10	761	1	5981	5	58	46
Sacarimb Sac 7.3 (6)	2548	0.44	—	—	566	53	—	1	15	2594	1.5	4	23	—	28		4	12
Sacarimb Sac 7.7 (5)	45,704	0.06	—	—	906	359	—	2	205	3652	63	110	351	36	12,150	157	81	770
Toroiaga Tga-1 (6)	763	7.16	1	—	1644	4	—	—	7	7751	93	—	—	—	—	—	1	4
In-1 low-In (3)	220	5.05	12	—	2368	273	—	—	698	8339	509	1384	109	—	155	6	2	5
In-1 high-In (7)	71	5.69	17	—	36,228	144	—	—	3102	8785	58,752	1486	10	—	104	42	1	19
In-1 high-Sn (8)	118	4.81	6	1	24,053	103	—	—	12054	9582	9660	11,703	35	—	1064	644	1	31
In-2 (4)	207	4.49	38	4	2615	191	3	1	1400	4507	2070	598	2010	5	3731	0.5	4	9
Skarn deposits																		
Majdanpek MD-20 (8)	3919	9.04	34	0.6	251	0.6	—	0.13	1.8	2898	56	0.4	0.1	—	0.5	0.5	0.8	76
OdF P43 low-Fe (9)	2618	1.77	151	0.4	181	0.2	—	0.1	15	6227	0.1	0.05	0.2	—	3240	31	0.6	3
OdF 3375 (6)	6758	0.6	2299	0.6	15	0.7	0.3	0.4	68	6763	1.9	0.1	0.1	0.18	12,230	140	0.8	10
OdF 3910b (8)	6042	3.01	302	2.3	268	0.4	2.6	0.2	6.8	5088	17	0.2	0.7	0.04	1539	13	1.1	4.4
OdF 54G (6)	2725	1.96	570	0.5	3785	0.2	0.7	0.3	5.6	5404	17	0.1	0.3	0.08	753	23	1.1	7.9
OdF St1 (6)	4627	6.04	25	0.6	486	1.7	0.3	0.3	4.3	5845	86	1.6	1.1	0.04	332	1	1.6	4.3
BB19CB (6)	967	0.13	1183	7.4	2893	0.3	—	0.03	20	5769	812	0.4	—	—	12	1	0.6	20
BB16C (6)	3359	1.29	504	6.2	53	1.5	—	0.11	1.4	7838	24	0.04	0.3	—	1.7	0.08	0.6	8

Continued

样品编号	Mn	Fe (%)	Co	Ni	Cu	Ga	As	Mo	Ag	Cd	In	Sn	Sb	Tl	Pb	Bi	Ge	Se
BB6 (8)	3827	1.3	599	11	244	1	0.3	0.1	8.5	7352	223	5.4	0.5	0.03	46	5.3	1.1	7.5
BB23 (10)	970	0.8	29	—	31	4	—	—	4	2262	29	—	—	—	—	—	1	120
VS 1b (6)	1643	2.86	8	0.3	13,122	2.8	0.2	0.1	18	5451	60	21	0.3	0.02	594	18	1.3	3.7
Bs7a (11)	298	0.28	9	—	1588	8	—	2	46	73,800	22	33	25	13	436	25	1	6
Bs7g (10)	668	1.36	13	1	978	22	2.2	—	107	8656	1	7	313	39	4100	5	10	4
Kamioka Kam-1 (8)	1380	2.04	230	3.2	3	0.1	—	—	14	5446	1	0.2	—	0.1	1345	303	0.6	61
Lefevre (CLY) L-12 (8)	3050	10.4	328	4.6	306	0.8	0.3	0.2	3.4	10,804	180	0.1	0.1	0.1	3.8	2.4	2.3	16
Konnerudkollen Ko99.2 (5)	545	0.43	1547	5.1	389	0.5	0.4	—	93	2449	7.6	0.1	—	0.3	3451	171	0.7	24
Stratabound deposits																		
TM low-Fe (10)	8.5	3.14	0.2	0.9	7.5	24	434	3.4	2.2	4720	0.1	2.1	62	53	3090	0.7	252	2.1
TM-high-Fe (12)	44	8.72	0.4	0.3	29	2.6	572	0.4	4.6	5434	0.2	3.9	11	158	1349	0.2	1081	1.7
Sinkholmen Znh1 (8)	2.3	0.3	0.1	—	1452	82	28	0.1	37	3916	0.5	3.8	24	—	15	0.3	4.6	15
Kapp Mineral KMi5 (10)	101	1.74	8.6	3.6	814	16	2.4	—	123	1011	2.1	16	33	—	1354	0.3	13	2.5
Hitra Hit-1 (8)	108	1.58	15	8	344	2.7	17	—	27	6938	0.2	0.8	102	—	160	0.1	1	1
VMS deposits																		
Vorta DMV (8)	530	0.19	—	—	382	96	—	58	6	4744	—	—	3.2	0.2	462	0.3	7	1.1
Eskay Creek P5 (12)	3265	0.49	0.04	0.8	770	148	211	3.1	535	3852	1.4	13	20,420	3.6	11,521	0.04	2.1	1.3
Sauda Sa-1 (10)	870	8.02	29	—	31	4	—	—	4	2262	29	—	—	—	—	—	1	119
Zinkgruvan Zn99.2 (5)	513	3.23	160	0.7	3.4	2.2	0.1	—	6.5	3812	0.3	0.1	1.2	—	43	0.1	1.1	0.1
Kaveltorp Kv99.1 (7)	30,032	9.86	11	1	1229	2.1	0.3	0.9	5.5	1660	4.6	0.6	0.2	0.1	1503	1	2.1	1.9
Marketorp Ma99.4 (8)	4104	9.69	170	0.2	4021	2.3	0.2	0.1	14	3250	26	0.3	—	—	12	23	3.5	33

Table 4. Concentrations for minor and trace elements in sphalerite samples of attached Table 1 (samples No. 41~119 of attached Table 1, ppm, except Fe)

表 4. 附表 1 闪锌矿样品主微量元素含量(附表 1 序号 41~119 的样品，ppm，Fe 除外)

样品编号	Ti	V	Cr	Mn	Fe (%)	Co	Ni	Cu	Zn	Ga	As	Ag	Cd	In	Sn	Sb	Tl	Pb	Bi	Ge	Se
Unknown deposits																					
3115X-37	—	—	—	0	8.58	—	—	39,900	523,600	—	600	100	2000	21,400	500	—	—	—	600	—	400
5497/3/28	—	—	—	600	10.30	—	—	33,800	477,100	—	1000	500	2200	55,900	600	—	—	—	500	—	600
8381-8	—	—	—	600	11.64	—	—	4000	534,000	—	800	500	2100	3700	800	—	—	—	1200	—	300
10428D-1-5	—	—	—	0	0.26	—	—	7100	645,800	—	300	500	1500	8800	500	—	—	—	0	—	0
14488-117	—	—	—	0	5.78	—	—	67,700	522,700	—	1500	500	3100	17,900	400	—	—	—	200	—	1000
Sample 1A	—	—	—	1690	9.91	179	—	66	560,000	—	—	5.7	945	—	—	—	—	—	—	—	—
Sample 1B	—	—	—	1630	9.86	164	—	123	519,000	—	—	4.3	963	—	—	—	—	—	—	—	—
Sample 2A	—	—	—	2310	8.47	124	—	86	575,000	—	—	9.9	341	—	—	—	—	—	—	—	—
Sample 2B	—	—	—	2250	8.83	128	—	63	581,000	—	—	5.5	361	—	—	—	—	—	—	—	—
Sample 3A	—	—	—	5770	10.90	442	—	87	549,000	—	—	4.4	632	—	—	—	—	—	—	—	—
Sample 3B	—	—	—	1890	9.83	489	—	55	571,000	—	—	3.7	842	—	—	—	—	—	—	—	—
Sample 4A	—	—	—	1280	5.16	89	—	42	610,000	—	—	10.9	757	—	—	—	—	—	—	—	—
Sample 4B	—	—	—	1130	5.08	92	—	22	597,000	—	—	10.3	813	—	—	—	—	—	—	—	—
Sample 5A	—	—	—	340	5.06	469	—	47,000	611,000	—	—	10.4	753	—	—	—	—	—	—	—	—
Sample 5B	—	—	—	270	3.75	456	—	21,600	514,000	—	—	3.3	805	—	—	—	—	—	—	—	—
Hydrothermal deposits																					
222(202)	—	—	—	2000	12.89	—	—	1900	511,400	700	—	—	5000	1600	—	—	—	—	—	—	—
50437-1A(5)	—	—	—	600	1.59	—	—	4200	625,500	900	—	—	10,300	—	—	—	—	—	—	—	—
50437-1B(25)	—	—	—	1700	11.34	—	—	1700	539,200	1000	—	—	3800	900	—	—	—	—	—	—	—
Zinnw1-5(19)	—	—	—	2100	3.29	—	—	2200	615,100	—	—	—	4800	700	—	—	—	—	—	—	—
1164	96	39	41	39	0.30	—	—	85	652,000	—	—	—	2270	111	—	—	—	—	—	—	—
1165bis	60	35	31	2150	10.19	—	—	436	544,800	—	—	—	3130	751	—	—	—	—	—	—	—

Continued

样品编号	Ti	V	Cr	Mn	Fe (%)	Co	Ni	Cu	Zn	Ga	As	Ag	Cd	In	Sn	Sb	Tl	Pb	Bi	Ge	Se
1168	95	39	35	42	0.05	—	—	—	660,900	—	—	—	990	129	—	—	—	—	—	—	—
1188	51	35	25	68	1.69	—	—	1100	625,100	—	—	—	4770	134	—	—	—	—	—	—	—
1189	104	43	35	57	1.56	—	—	604	636,300	—	—	—	3150	142	—	—	—	—	—	—	—
1293	89	46	30	33	0.27	—	—	339	643,900	—	—	—	2550	142	—	—	—	—	—	—	—
1303	46	40	30	43	1.15	—	—	32	645,900	—	—	—	3220	205	—	—	—	—	—	—	—
1212	80	38	42	13,420	0.29	—	—	73	640,000	—	—	—	3540	—	—	—	—	—	—	—	—
1215	59	33	42	51	1.36	—	—	78	636,500	—	—	—	1430	129	—	—	—	—	—	—	—
1227	55	33	34	8870	0.28	—	—	30	652,000	—	—	—	4440	51	—	—	—	—	—	—	—
1257	68	40	27	3620	0.35	—	—	107	648,200	—	—	—	4110	130	—	—	—	—	—	—	—
MVT deposits																					
47975	55	38	32	75	9.51	—	—	—	595,500	—	—	—	3310	197	—	—	—	—	—	—	—
HZF-1086	—	—	—	111	3.43	0.04	0.16	602	—	5	—	28.8	3059	—	0.11	64	0.04	13	—	165	—
HZF-1062	—	—	—	58.8	1.38	—	—	157	—	0.81	—	28.5	1689	—	0.81	17.5	0.16	13.1	—	52.3	—
HZF-1065	—	—	—	119	1.56	0.02	—	102	—	6	—	10.8	1612	1.9	4.1	4.7	—	3.7	—	29.9	—
B-10	—	—	—	9.1	1.38	—	—	—	—	9.8	—	20.4	13,963	0.18	1.6	—	0.6	395	—	44.3	0.7
B-6	—	—	—	6	0.75	—	—	14.40	—	7.8	—	5.6	9000	0.05	0.74	—	0.41	211	—	29.7	0.35
H-22	—	—	—	75.7	1.39	—	—	124	—	16.1	—	5	7028	0.034	2.4	—	12.1	835	0.02	182	0.43
M-1	—	—	—	40.1	0.91	0.82	—	156	—	3.3	—	4.3	9465	—	0.27	87.9	8.8	972	0.07	26.8	—
M-11	—	—	—	281	0.07	4.30	—	4.4	—	0.83	—	4.2	15,472	—	0.12	1.9	8.6	386	0.06	2.8	0.61
BP368-263.9	—	—	—	101	1.39	84	14	142	—	84	—	3.7	3235	—	—	—	—	3	—	45	—
CR-5R	—	—	—	201	1.80	255	29	959	—	118	—	12.5	3292	—	33	—	—	38	—	91	—
CR-24.8R	—	—	—	124	1.69	264	10	1377	—	73	—	11.9	3103	—	—	—	—	107	—	34	—
S-274	—	—	—	123	1.51	104	12	301	—	119	—	6.5	3989	—	—	—	—	5280	—	14	—
B8-1	—	—	—	157	3.54	15	15	7	—	1.9	—	1.4	4833	—	—	—	—	22	—	0.02	—
Ba-5	—	—	—	407	3.59	18	37	10	—	1.5	—	6.1	4456	—	—	—	—	270	—	0.06	—

Continued

样品编号	Ti	V	Cr	Mn	Fe (%)	Co	Ni	Cu	Zn	Ga	As	Ag	Cd	In	Sn	Sb	Tl	Pb	Bi	Ge	Se
B8-3	—	—	—	209	3.44	14	11	8	—	2	—	1.7	4930	—	—	—	—	7	—	0.05	—
GAP-5	—	—	—	174	3.41	19	20	78	—	7.8	—	6	5005	—	54	—	—	28	—	0.2	—
GBP-2	—	—	—	105	2.76	67	13	229	—	44	—	8.3	5774	—	—	—	—	26	—	72	—
GBP-1	—	—	—	78	2.36	68	12	14	—	7.2	—	2.8	4292	—	—	—	—	68	—	2.2	—
GAP-4	—	—	—	118	3.19	27	18	128	—	9.5	—	9	5116	—	—	—	—	20	—	4.7	—
EH16-106.7	—	—	—	144	2.66	89	14	456	—	32	—	7.4	4277	—	—	—	—	207	—	35	—
P1-8	—	—	—	502	0.32	3	6	58	—	52	—	0.5	250	—	—	—	—	129	—	1.1	—
P91-45.6	—	—	—	893	0.37	18	9	167	—	35	—	9.6	699	—	—	—	—	41,016	—	72	—
P1-107.4	—	—	—	517	1.12	3	14	259	—	37	—	0.9	4650	—	—	—	—	1674	—	0.5	—
P1-101.7	—	—	—	577	0.62	3	5	73	—	78	—	0.4	2486	—	—	—	—	5	—	0.09	—
Sandstone-hosted deposits																					
M	—	—	—	538	0.06	17.80	0.64	5.60	—	0.96	—	30.4	6561	—	—	2	17.3	483	—	8.8	—
Jind-150	—	—	—	124	0.17	3.60	—	1406	—	3.4	—	49.8	9037	—	—	4.9	12.6	4145	—	3.4	—
Jind-148	—	—	—	62.3	0.07	—	—	—	—	1.3	—	4	35,468	—	—	—	6.7	159	—	20.8	—
Jind-155-26	—	—	—	11.7	0.23	0.33	—	97.90	—	4.4	—	4.4	20,692	0.006	0.23	46.3	21.3	913	0.04	12.4	0.5
SEDEX deposits																					
DBS-1	—	—	—	1762	11.03	0.19	—	155	—	38.3	—	21.9	5580	122	5.5	3	—	51.7	—	3.1	—
DBS-2	—	—	—	2347	11.99	5.40	—	1418	—	12.8	—	31.2	5475	300	19	2.2	—	14.9	—	3.3	—
DBS-6	—	—	—	2425	12.08	1.30	—	946	—	33.9	—	54.7	5779	285	13.1	7.3	—	9.2	—	3.5	—
BNC-3	—	—	—	3883	13.46	6.30	—	2254	—	14.1	—	38.8	8195	110	1129	2.9	—	2.5	—	3.4	—
BNC-10	—	—	—	3945	15.42	0.11	—	5702	—	7.6	—	95.1	5568	21.9	660	8.3	—	18.3	—	5.4	—
Skarn deposits																					
1	65	34	28	31	0.14	—	—	72	656,400	—	—	—	810	140	—	—	—	—	—	—	—
1206	99	29	32	33	0.23	—	—	103	646,900	—	—	—	3500	130	—	—	—	—	—	—	—
1210	87	27	22	84	1.89	—	—	80	636,300	—	—	—	5700	132	—	—	—	—	—	—	—

Continued

样品编号	Ti	V	Cr	Mn	Fe (%)	Co	Ni	Cu	Zn	Ga	As	Ag	Cd	In	Sn	Sb	Tl	Pb	Bi	Ge	Se
1211	26	29	30	5890	6.32	—	—	42	580,000	—	—	—	4320	98	—	—	—	—	—	—	—
1276	45	35	42	2930	2.34	—	—	43	628,600	—	—	—	1540	56	—	—	—	—	—	—	—
HTP-27	—	—	—	2832	3.72	110	—	9.70	—	0.87	—	5.7	4240	0.01	0.11	1.9	—	3.5	0.01	2.7	22
HTP-174	—	—	—	5115	10.03	78.30	—	1753	—	0.16	—	12.7	5847	0.13	—	9.3	—	23.3	0.53	3	16.5
HTP-163	—	—	—	1273	2.08	449	0.22	104	—	0.57	—	6.4	4125	0.003	—	2.6	—	85.3	3.2	2.8	55.7
LZY-47	—	—	—	1462	4.39	434	—	41.70	—	0.32	—	4.6	2280	0.11	0.12	7	—	352	14.8	2.9	117
LZY-29	—	—	—	654	9.92	244	—	254	—	0.56	—	8.6	1967	0.05	3	—	—	15.4	—	3.1	1.5
LZY-61	—	—	—	1093	5.73	411	0.30	13.80	—	0.12	—	4.7	2194	0.007	0.13	—	—	3.3	—	3	16.1
VMS deposits																					
22551	63	45	35	36	0.22	—	—	211	657,400	—	—	—	1130	118	—	—	—	—	—	—	—
LC-9	—	—	—	2734	12.82	0.43	—	180	—	15.9	—	6.4	8673	183	5.7	—	—	43.1	—	3.7	—
LC-19	—	—	—	3465	14.21	0.58	—	251	—	41.2	—	6.3	8769	293	10.3	—	—	1.7	—	3.7	2.2
LC-18	—	—	—	3225	12.41	2	0.31	436	—	17.5	—	8	8825	138	6	1.6	0.68	18.6	—	5.4	—

4. 实验结果

38 件闪锌矿样品的主微量元素含量分析结果见表 2。其余文献中收集的样品结果见表 3 (数据来自 CODES [10]，采用原位 LA-ICPMS 分析法)及表 4 (数据来自文献(附表 1)，主要采用电子探针或原位 LA-ICPMS 分析法，其中样品“Sample 1B，2B，3B，4B，5B”使用的是 SN-ICP-SFMS 分析法)。本次在墨尔本大学测试的样品以及上述表 4 中的 5 件样品得到的是闪锌矿粉末元素的含量，而其余通过电子探针或原位 LA-ICPMS 测试得到的结果可能会受到样品内部化学分区的影响。原位分析方法可能对某些元素的分析不完整，如 Pb、Bi，这些元素可能存在矿物包裹体中。但是，对于大部分元素来说(如 In，Mn，Cd，Ge，Ga，Co 等)，在测试点的范围内会均匀的分布，因此这两种方法都应该是可靠的[10]。

分析结果显示单个元素的含量可能超过几个数量级。元素的分布情况将在下文进行分析，首先根据矿床成因类型及矿床工业类型进行分析，然后通过元素组合进行分析。在分析结果的过程中，Pb-Zn、Zn 和 Zn-Pb 矿床统称为 Pb-Zn 矿床；Pb-Zn-Cu、Zn-Pb-Cu 矿床统称为 Pb-Zn-Cu 矿床；Pb-Zn-Ag、Zn-Pb-Ag 矿床统称为 Pb-Zn-Ag 矿床；Au、Au-Ag 矿床统称为 Au 矿床；Cu、Cu-Au、Cu-Zn-Pb 矿床统称为 Cu 矿床；Ag、Ag-Au、Ag-Pb 矿床统称为 Ag 矿床。

4.1. 热液矿床(Hydrothermal Deposits)

表 2 中有四件闪锌矿样品(M35909A, M35909B, M45431, M45751)来自热液矿床，测试结果显示其 In 含量远高于 Ga，尤其是 M45431 富含 In (66.61 ppm)，同时也富含 As (1328.94 ppm)、Cu (1527.13 ppm)、Ag (18.83 ppm)、Pb (387.32 ppm)。由于 M45431 来自锡矿床，其 Sn 含量也非常高(1133.5 ppm)。其余三个样品来自 Pb-Zn-Ag 矿床，但是 Pb、Ag、Cu 含量远低于 Wheal Jane 锡矿床。

表 3 中的热液矿床可分为 Au 矿床和 Zn-Pb-Cu 矿床，前者 Ga 含量高于 In，后者正好相反。但是 Zn-Pb-Cu 矿床中 Ga、In，以及 Cu、Ag、Sn 的含量相对高于 Au 矿床。来自 Au 矿床的两件闪锌矿样品(Mag-8 和 Sac 7.3)基本不含 In。相反，它们富含 Ga 和 Ge，而 Mag-8 富含 As。

表 4 中，热液矿床中 In 含量高。而 Ag 矿床中 Cu 含量相对于 Pb-Zn 或 Pb-Zn-Cu 矿床非常高。

4.2. 矽卡岩型矿床(Skarn Deposits)

表 2 中矽卡岩型矿床结果显示 In 含量高于 Ga。尤其是 M9317 (来自锡矿床，Sn 含量为 7464.12 ppm) In 含量很高(1378.19 ppm)，同时 Cu (8781.88 ppm)，Ag (141.91 ppm)，Pb (59082.82 ppm)，Sb (20139.48 ppm)含量也较高，As (3.82 ppm)含量中等。在所有的结果中，In 都显示与 Cu 具体很强的相关性。

表 3 中来自 Majdanpek Zn-Pb 矿床的闪锌矿样品富 Fe，同时 In 含量很高，而 Ag、Pb、Bi 含量较低。来自 Ocna de Fier 的闪锌矿 Fe 含量较低，而 Cu、Pb、Bi 含量范围变化较大。Co 含量值在 Fe 含量高时(6.04%)其含量低(25 ppm)，而 Fe 含量低时(0.6%)其含量则高(2299 ppm)。样品 OdF 3375 中 Co 含量为 2300 ppm，是所知闪锌矿中 Co 含量最高的数值。采自 Baita Bihor 的四件样品 Ga 含量非常低(全部低于 4 ppm)。采自铜矿化的样品 BB19CB 中 In (812 ppm)和 Cu (2893 ppm)含量很高，Se、Ag 含量异常。

表 4 采自 Zn-Pb 矿床的 HTP 与 LZY 系列样品 In 含量很低(均低于 0.13 ppm)，而 Ga(0.12-0.87 ppm)、Co (78.3~449 ppm)含量相对较高。相反，其他样品 In 含量很高，而 Cu 含量相对稳定。在所有 HTP 与 LZY 系列样品中，Ga 含量与 Co 负相关。

4.3. 网脉状矿床(Stockwork Deposits)

表 2 中采自 Ni 矿床的闪锌矿样品(M37225) Co 含量很高(935.13 ppm)，也是表 2 中最高的，相对于此类型矿床的其他样品来说，其 Ni (8.74 ppm)、Ga (17.63 ppm)、In (36.63 ppm)含量也相对较高。此项研究

中唯一的 U-Th-REE 矿床，其闪锌矿样品 Ga 和 In 含量非常低，而 Nb 和 Ti 含量高。样品 M39582A 的 Nb 含量(18.79 ppm)和样品 M39582B 的 Ti 含量(40.15 ppm)在表 2 中是最高的。Ravenswood 网脉状 Au 矿床(M9306)富含 Cu (1367.28 ppm)，As (576.18ppm)，Ag (301.69 ppm)，Sn (117.46 ppm)，Sb (62.16 ppm)和 Pb (47449.05 ppm)，这也是本文网脉状矿床中这 6 种元素含量最高的值。样品 M41383 (Ag-Au 矿床)富集 Ag (16.22 ppm)及 Cd (3307.29 ppm，是网脉状矿床中 Cd 含量最高值)。

4.4. 层控型矿床(Stratabound Deposits)

除去 M50250 采自 Ag-Pb 矿床外，表 2 中此类型矿床的其他样品均采自 Pb-Zn 或 Pb-Zn-Ag 矿床。M50250 贫 Cu、Ga、In，富 Ag、Pb。其余 5 件样品 Ga、In 含量高于 M50250。样品 M9323 采自 Wheal Ellen Zn-Pb-Ag 矿床，其 Ga 含量(496.58 ppm)是六件样品中最高的。

表 3 中采自 Tres Marias 的闪锌矿样品分为富 Ge-Fe 和贫 Ge-Fe 两类。富 Ge 的部分同时富 As 和 Tl；而贫 Ge 的样品贫 As 和 Tl，但是 Sb 含量高。

大部分层控型矿床样品中普遍 Ga、In 含量高。

4.5. 海相火山成因块状硫化物矿床(VMS Deposits)

表 2 中，采自澳大利亚南部 Talisker Ag-Pb 矿的样品 M9321，其 Ag (353.48 ppm)和 Pb (119,154.65 ppm)含量非常高，同时 In (82.49 ppm)和 Sb (133.13 ppm)含量也相对较高，而 Cu 含量低于其余两件样品(为 Zn-Pb-Cu 矿床)。

表 3 中样品 Vorta DMV 富集 Mo (58 ppm)及 Ga (96 ppm)。样品 Eskay Creek P5 中元素 Ga、Pb、Sb、Ag、Cu、As、Tl 值都非常高。

4.6. 斑岩型、喷流沉积型矿床(SEDEX Deposits)

表 4 中，采自 BNC 锡矿床的样品(BNC-3 和 BNC-10)，其 Sn 含量非常高(分别为 11,229 ppm 和 660 ppm)。在 SECEX 矿床中，样品 In 含量一般都比 Ga 高一个数量级。

4.7. 密西西比河谷型矿床(MVT Deposits)

本文采自 MVT 矿床的样品均为 Pb-Zn 或 Pb-Zn-Ag 矿床。其 Ga 含量均比 In 含量高一至两个数量级。

表 4 收集的数据中所有的样品均为 Pb-Zn 矿床，其 Ga、Ag、Cu 和 Pb 的含量变化范围很大。几乎所有样品都是贫 Fe 闪锌矿，其 Fe 含量低于 3.6% (样品 47975 除外，为 9.51%)。

4.8. 单一元素的分布情况

不同类型矿床中元素的变化可在以下直方图中显示出来。

图 1 为 Ga 含量直方图。所有样品的 Ga 含量平均值为 59.81 ppm (n = 123)。单一样品的浓度主要集中在 1~100 ppm (80/123，图 1(A))。Ga 富集在热液矿床中(其中有 8 件样品含量集中在 100~1000 ppm，图 1(B1))。矽卡岩型与网脉状矿床 Ga 含量较低(大部分低于 10 ppm，图 1(B2)，图 1(B3))。图 1(C1)~(C7)主要显示 Ga 在不同工业类型矿床的分布情况。Pb-Zn-Cu 和 Ag 矿床富 Ga (大部分超过了 100 ppm，图 1(C2)，图 1(C7))，而 Cu 矿床中 Ga 含量最低(最低为 0.054 ppm，图 1(C5))。

In 含量平均值非常高(1585.18 ppm, n = 121)。一半以上样品 In 含量在 10 到 1000 ppm 之间(图 2(A))。热液矿床、矽卡岩型矿床、VMS 和 SEDEX 型矿床 In 含量高(图 2(B1)、图 2(B2)、图 2(B5)、图 2(B6))，其中热液矿床具有 In 最高含量值 58,752 ppm (图 2(B1))。以矿床工业类型进行分析，Sn 矿床含 In 量最高(图 2(C6))，其次是 Pb-Zn-Cu 矿床(图 2(C2))。

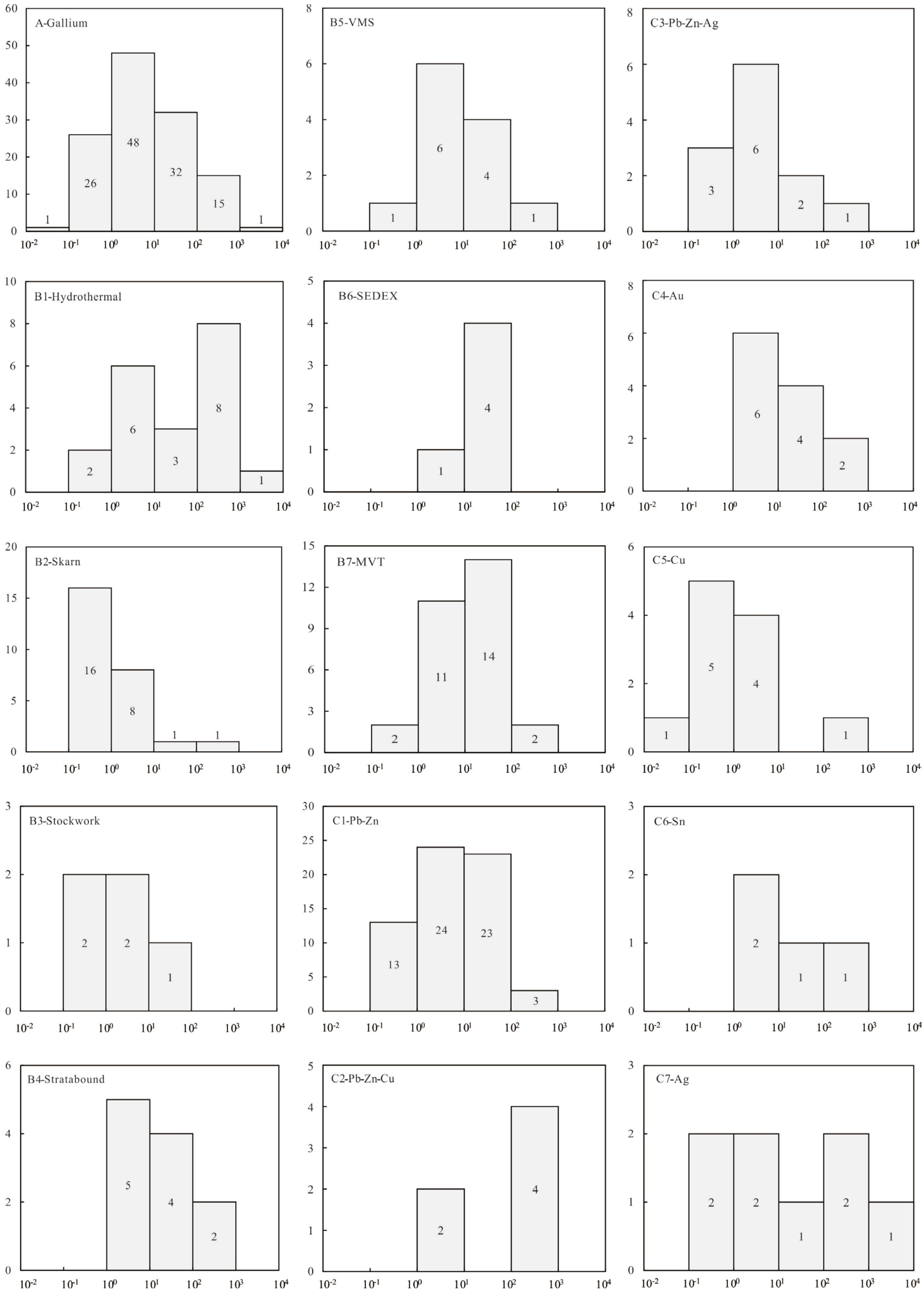

Figure 1. Histograms showing the distribution of Ga in sphalerite; (A: in all the samples, B1~B7: in different genetic types, C1~C7: in different industrial types, X-coordinate: concentrations in ppm, Y-coordinate: frequency)

图 1. 闪锌矿中 Ga 含量直方图。(A：所有样品，B1~B7：不同矿床成因类型，C1~C7：不同矿床工业类型，X 轴：含量/ppm，Y 轴：频率)

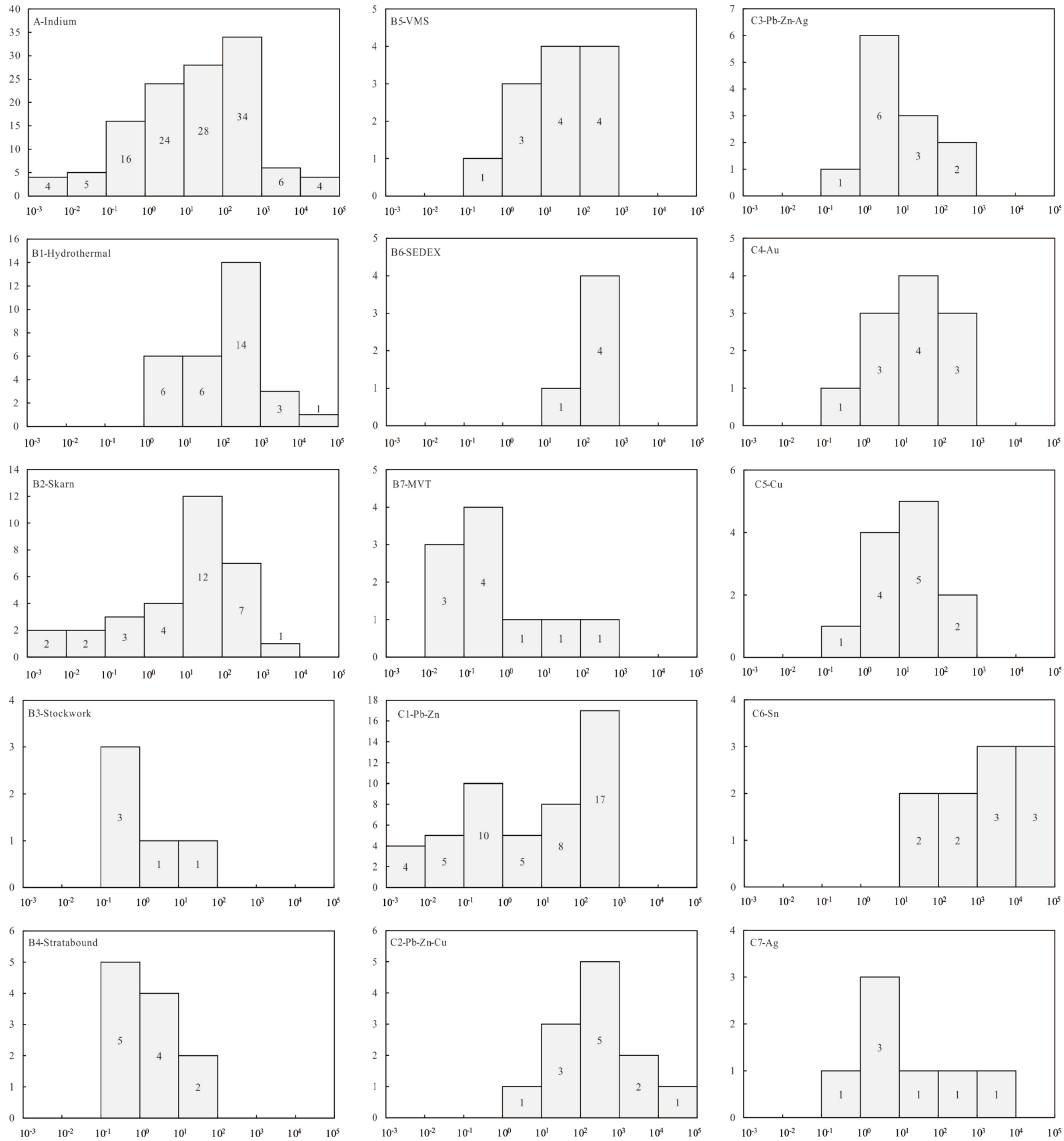

Figure 2. Histograms showing the distribution of In in sphalerite. (A: in all the samples, B1~B7: in different genetic types, C1~C7: in different industrial types, X-coordinate: concentrations in ppm, Y-coordinate: frequency)

图 2. 闪锌矿中 In 含量直方图。(A：所有样品，B1~B7：不同矿床成因类型，C1~C7：不同矿床工业类型，X 轴：含量/ppm，Y 轴：频率)

Ga 富集在 Ag 矿床中，因此作者对不同类型矿床中 Ag 的分布进行了讨论。Ag 含量集中于 0.1~10 ppm (48%，n = 135，图 3(A))。且 Ag 含量分布与 Ga 类似。Ag 在热液矿床中的含量分布最广泛(图 3(B1))。而在其他几种类型的矿床中含量基本都不超过 100 ppm (图 3(B2)~(B7))。Pb-Zn-Cu 矿床中的 Ag 含量(12,054 ppm)最高(图 3(C2))，且高于 Pb-Zn-Ag 和 Ag 矿床(图 3(C3)、图 3(C7))。

Sn 矿床中 In 含量最高，因此，对 Sn 含量分布进行了分析。结果显示，在大部分样品中，Sn 含量普

遍较低(81% < 100 ppm, n = 102)，尤其是矽卡岩型矿床(图 4(A)、图 4(B2))。Sn 在 Pb-Zn-Cu、Sn 和 Ag 矿床中的含量比较高(含量最高大于 1000 ppm，图 4(C2)、图 4(C6)、图 4(C7))。

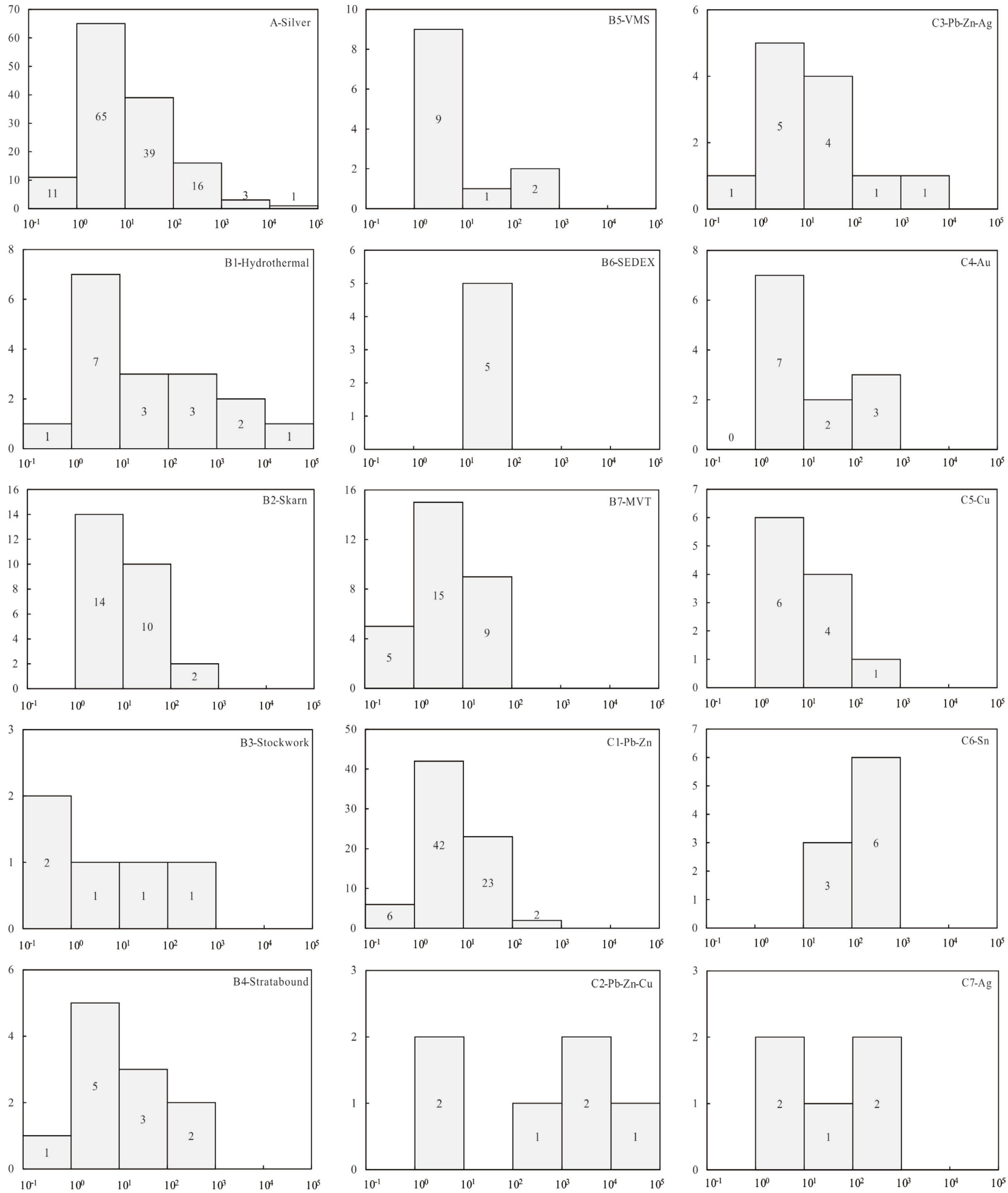

Figure 3. Histograms showing the distribution of Ag in sphalerite. (A: in all the samples, B1~B7: in different genetic types, C1~C7: in different industrial types, X-coordinate: concentrations in ppm, Y-coordinate: frequency)

图 3. 闪锌矿中 Ag 含量直方图。(A：所有样品，B1~B7：不同矿床成因类型，C1~C7：不同矿床工业类型，X 轴：含量/ppm，Y 轴：频率)

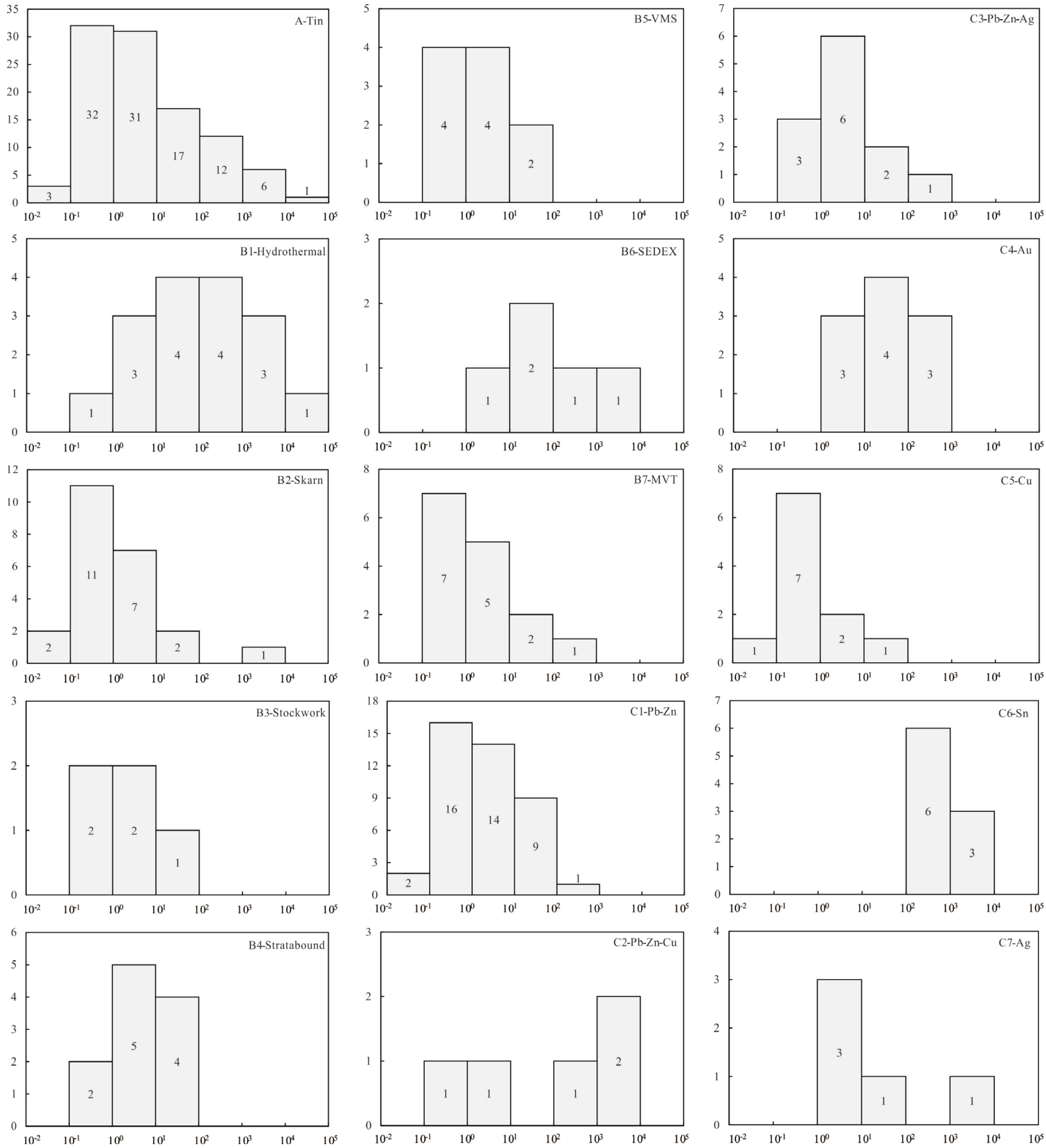

Figure 4. Histograms showing the distribution of Sn in sphalerite. (A: in all the samples, B1~B7: in different genetic types, C1~C7: in different industrial types, X-coordinate: concentrations in ppm, Y-coordinate: frequency)

图 4. 闪锌矿中 Sn 含量直方图。(A：所有样品，B1~B7：不同矿床成因类型，C1~C7：不同矿床工业类型，X 轴：含量/ppm，Y 轴：频率)

5. 讨论

5.1. 不同成因类型矿床闪锌矿中 Ga 和 In 的分布情况

作者计算了不同成因类型矿床闪锌矿中 Ga 和 In 含量的平均值，如图 5。Ga 在热液矿床闪锌矿中的含量最高，其次是层控型矿床。而 In 同样在热液矿床闪锌矿中含量最高，其次是 SECEX 型和矽卡岩型

矿床。由于热液矿床是一种相对广泛的成因类型，因此这类矿床中闪锌矿 Ga 和 In 含量均很高。

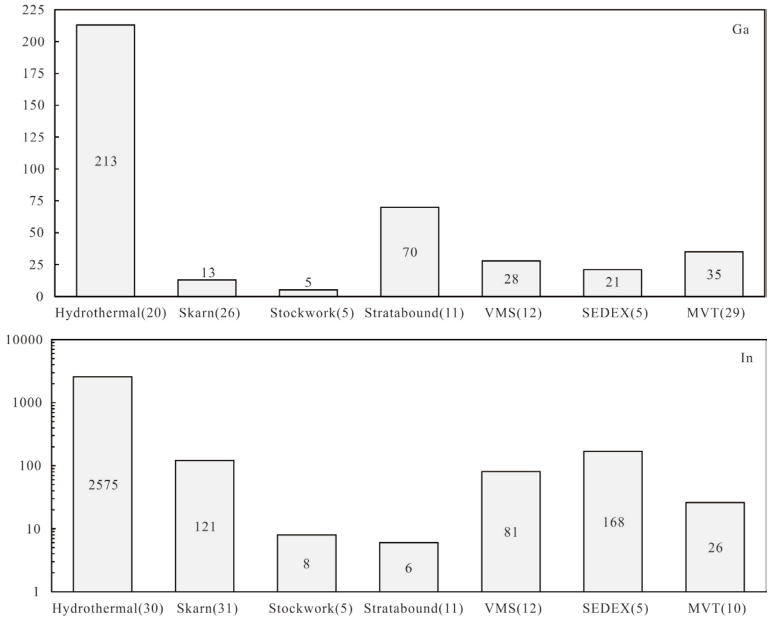

Figure 5. Histograms showing the mean concentrations (in ppm) of Ga and In in sphalerite of different genetic types (with the number of samples in the parenthesis)
图 5. 不同成因类型矿床闪锌矿中 Ga 和 In 的分布直方图(ppm，括号中为样品数)

5.2. 不同工业类型矿床闪锌矿中 Ga 和 In 的分布情况

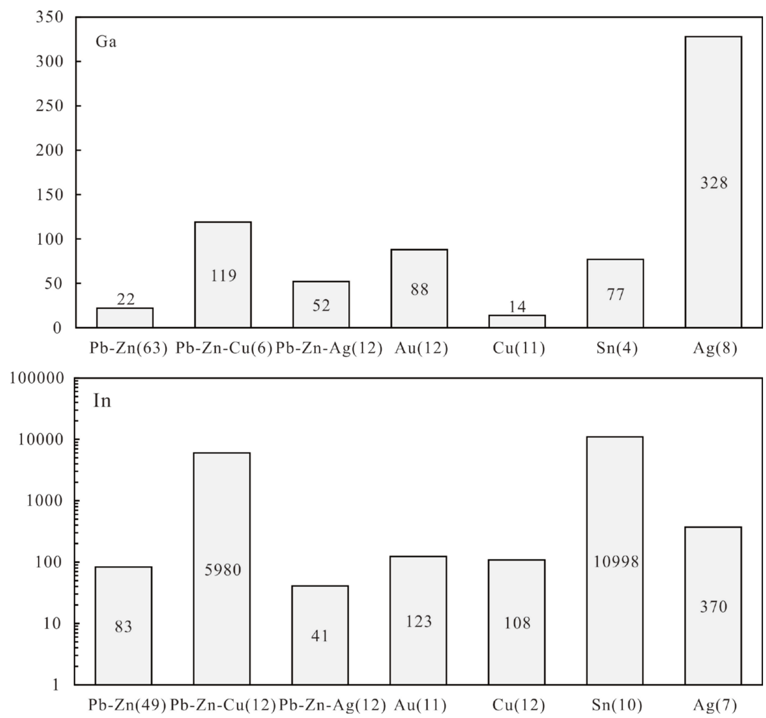

Figure 6. Histograms showing the mean concentrations (in ppm) of Ga and In in sphalerite of different industrial types (with the number of samples in the parenthesis)
图 6. 不同工业类型矿床闪锌矿中 Ga 和 In 的分布直方图(ppm，括号中为样品数)

作者计算了不同类型矿产闪锌矿中 Ga 和 In 含量的平均值，如图 6。Ga 在 Ag 矿床闪锌矿中的含量明显最高，其次是 Pb-Zn-Cu 矿床。而 In 在 Sn 矿床闪锌矿中含量最高，其次是 Pb-Zn-Cu 矿床。Pb-Zn-Cu、Au、Sn 和 Ag 四类矿产普遍含 Ga 和 In 高。

5.3. 元素相关性与置换

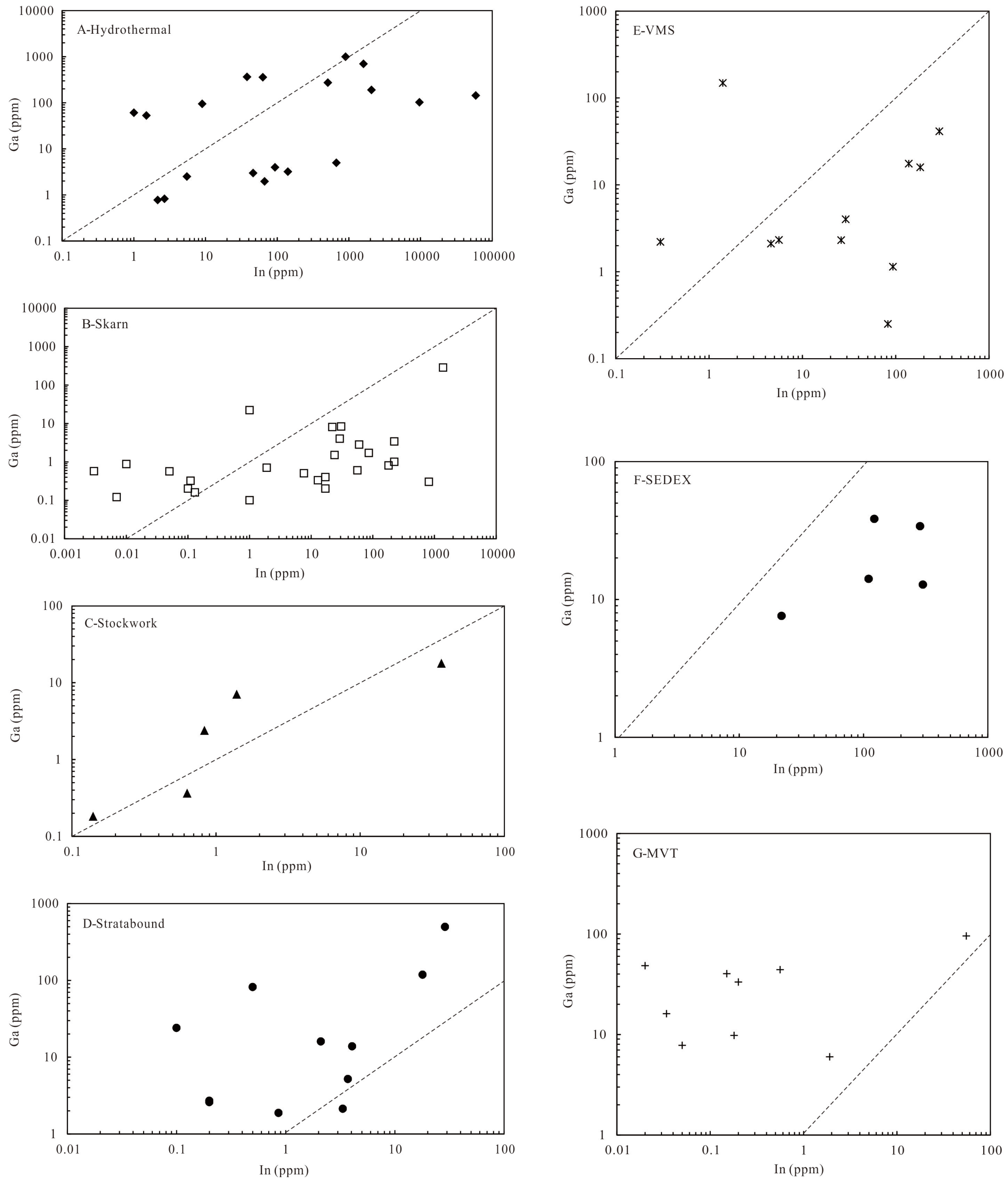

Figure 7. Correlation plots of Ga vs. In in sphalerite from different genetic types. Dashed lines represent 1:1 correlations between concentrations (ppm)

图 7. 不同成因类型矿床闪锌矿中 In-Ga 关系图(虚线 Ga/In = 1:1)

不同成因类型矿床中 Ga/In 分布情况如图 7。有些矿床类型 Ga/In 趋势明显。在 SEDEX 矿床中 Ga/In < 1 (图 7(F))，热液型、矽卡岩型、VMS 矿床中大部分样品的 Ga/In < 1 (图 7(A)，图 7(B)，图 7(E))。而在 MVT 与层控型矿床中 Ga/In > 1 (图 7(G)，图 7(D))。

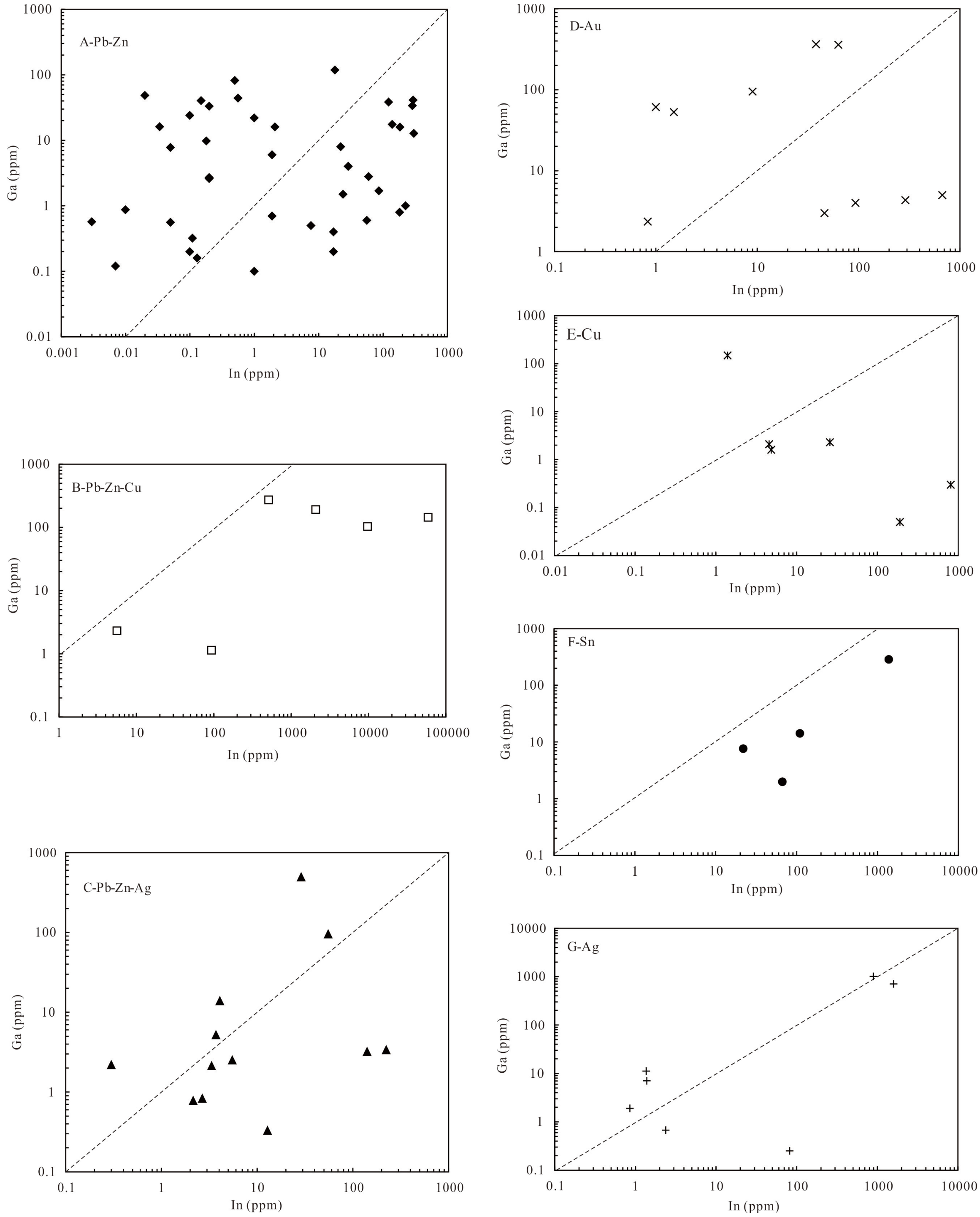

Figure 8. Correlation plots of Ga vs. In in sphalerite from different industrial types. Dashed lines represent 1:1 correlations between concentrations (ppm)
图 8. 不同工业类型矿床闪锌矿中 In-Ga 关系图(虚线 Ga/In = 1:1)

图 8 显示的是在不同工业类型矿床闪锌矿中 Ga/In 的分布情况。在不同工业类型矿床中 Ga/In 的趋势不是非常明显，大部分样品点比较分散。但是 Pb-Zn-Cu、Cu 和 Sn 矿产闪锌矿大多数样品 Ga/In < 1，表明三类矿产中 In 含量大于 Ga。

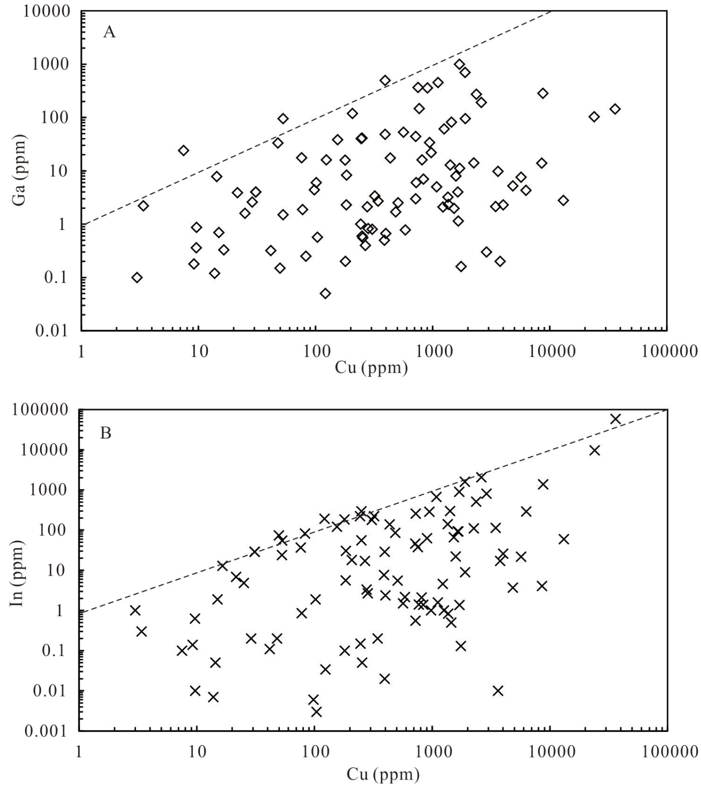

Figure 9. Correlation plots of (A) Ga vs. Cu, and (B) In vs. Cu in sphalerite from the total dataset. Dashed lines represent 1:1 correlations between concentrations (ppm)

图 9. 闪锌矿样品中 Cu-Ga(A)与 Cu-In(B)关系图(虚线 Ga/In = 1:1)

Ga 和 In 都与 Cu 有显著的正相关关系(图 9)，缘于$(Ag, Cu)^+ + Ga^{3+} \leftrightarrow 2Zn^{2+}$ [10]和 $Cu^+ + In^{3+} \leftrightarrow 2Zn^{2+}$ [3] [10]的置换机制。In/Cu 相关性远低于 1，可能是由于某些样品中黄铁矿的存在造成的[77]。$Cu^+ + In^{3+} \leftrightarrow 2Zn^{2+}$对 In 的富集非常重要，可形成不同颜色的条带状硫铟铜矿($CuInS_2$)，可以很容易通过显微镜在闪锌矿晶体中发现[3]。

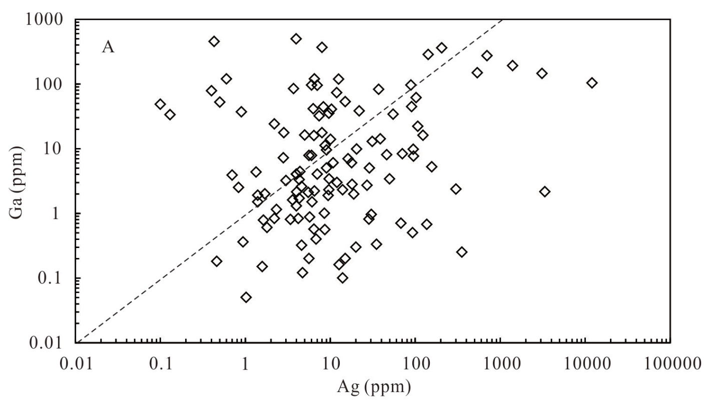

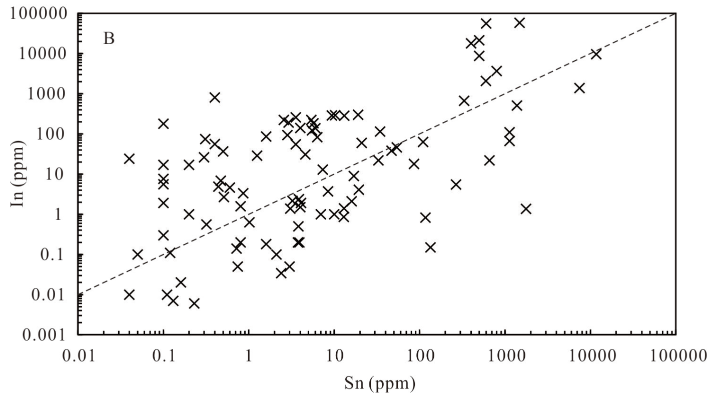

Figure 10. Correlation plots of (A) Ga vs. Ag, and (B) In vs. Sn in sphalerite from the total dataset. Dashed lines represent 1:1 correlations between concentrations (ppm)
图 10. 闪锌矿样品中 Ag-Ga(A)与 Sn-In(B)关系图(虚线 Ga/In = 1:1)

Ag 矿床中富 Ga，且 Sn 矿床中富 In，Ga 和 Ag、In 和 Sn 的相关性如图 10 所示。Ga 与 Ag 呈现正相关，证明$(Ag, Cu)^{+} + Ga^{3+} \leftrightarrow 2Zn^{2+}$置换的存在[10]。而 In 与 Sn 的正相关关系则是闪锌矿－黄锡矿固溶体存在的证据[10]。

Ga 与 Co 呈现明显的负相关性(图 11(A))。可见富 Co 的闪锌矿其 Ga 含量低，但是还未找到相关的置换机制。而 In 与 Zn 的负相关性(图 11(B))也是由于$Cu^{+} + In^{3+} \leftrightarrow 2Zn^{2+}$置换机制的存在。

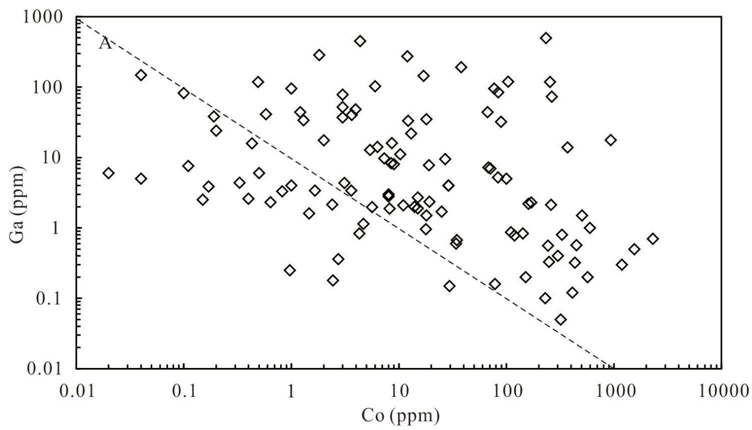

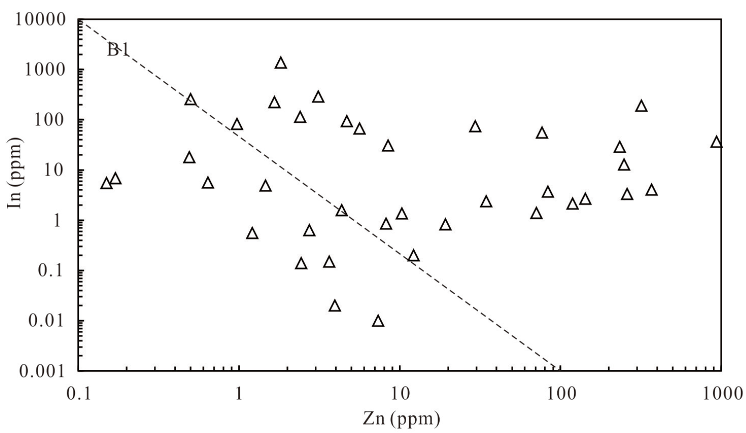

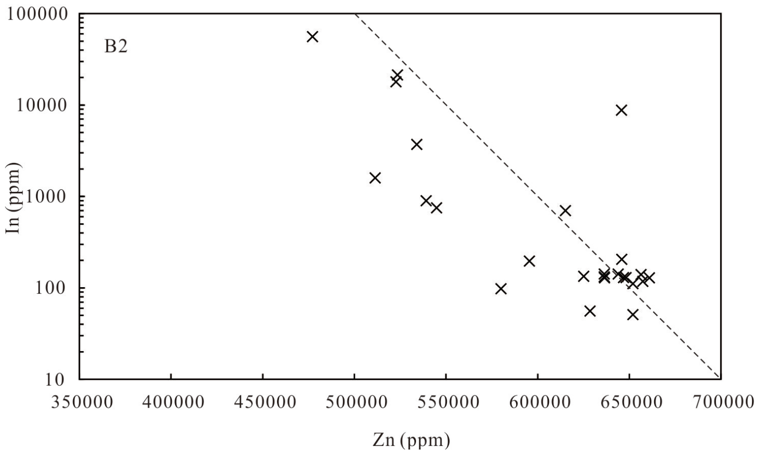

Figure 11. Correlation plots of (A) Ga vs. Co, and (B) In vs. Zn in sphalerite from the total dataset. Dashed lines represent (A)-1:1, (B1)-200:1, (B2)-1:2 correlations between concentrations (ppm)

图 11. 闪锌矿样品中 Co-Ga (A)与 Zn-In (B)关系图。(虚线表示(A)-1:1，(B1)-100:1，(B2)-1:2 的相关性)

6. 结论

1) 热液矿床中富集 Ga 和 In。Ga 还富集在层控型矿床中，而 SEDEX 和矽卡岩型矿床 In 含量较高。

2) Ag 矿床富集 Ga，而 Sn 矿床中 In 含量较高。Ga 与 Ag、In 与 Sn 的正相关性分别证明了置换机制 $(Ag, Cu)^{+} + Ga^{3+} \leftrightarrow 2Zn^{2+}$与闪锌矿－黄锡矿固溶体的存在。

3) Ga/In 比率可以用来判断矿床成因类型：Ga/In > 1 为层控型及 MVT 矿床；Ga/In ≈ 1 为网脉状矿床；Ga/In < 1 为热液、矽卡岩型、VMS 和 SEDEX 矿床。

4) Ga、In 与 Cu 的正相关性，缘于$(Ag, Cu)^{+} + Ga^{3+} \leftrightarrow 2Zn^{2+}$和 $2Zn^{2+} \leftrightarrow Cu^{+} + In^{3+}$置换机制的存在。

参考文献

[1] Axelsson, M.D. and Rodushkin, I. (2001) Determination of Major and Trace Elements in Sphalerite Using Laser Ablation Double Focusing Sector Field ICPMS. *Journal of Geochemical Exploration*, **72**, 81-89. https://doi.org/10.1016/S0375-6742(00)00166-7

[2] Viets, J.G., Hopkins, R.T. and Miller, B.M. (1992) Variations in Minor and Trace Metals in Sphalerite from Mississippi Valley-Type Deposits of the Ozark Region; Genetic Implications. *Economic Geology*, **87**, 1897-1905. https://doi.org/10.2113/gsecongeo.87.7.1897

[3] Benedetto, R.D., Bernardini, G.P., Costagliola, P., Plant, D. and Vaughan, D.J. (2005) Compositional Zoning in Sphalerite Crystals. *American Mineralogist*, **90**, 1384-1392. https://doi.org/10.2138/am.2005.1754

[4] Moskalyk, R.R. (2003) Gallium: The Backbone of the Electronics Industry. *Minerals Engineering*, **16**, 921-929. https://doi.org/10.1016/j.mineng.2003.08.003

[5] Carrillo-Rosúa, J., Morales-Ruano, S. and Hach-Alí, P.F. (2008) Textural and Chemical Features of Sphalerite from the Palai-Islica Deposit (SE Spain): Implications for Ore Genesis and Color. *Neues Jahrbuch Für Mineralogie Abhandlungen Journal of Mineralogy & Geochemistry*, **185**, 63-78. https://doi.org/10.1127/0077-7757/2008/0109

[6] Höll, R., Kling, M. and Schroll, E. (2007) Metallogenesis of Germanium—A Review. *Ore Geology Reviews*, **30**, 145-180. https://doi.org/10.1016/j.oregeorev.2005.07.034

[7] Alfantazi, A.M. and Moskalyk, R.R. (2003) Processing of Indium: A Review. *Minerals Engineering*, **16**, 687-694. https://doi.org/10.1016/S0892-6875(03)00168-7

[8] Sinclair, W.D., Kooiman, G.J.A., Martin, D.A. and Kjarsgaard, I.M. (2006) Geology, Geochemistry and Mineralogy of Indium Resources at Mount Pleasant, New Brunswick, Canada. *Ore Geology Reviews*, **28**, 123-145. https://doi.org/10.1016/j.oregeorev.2003.03.001

[9] Gatterer, A. (1941) Untersuchungen über die Nebenbestandteile von Erzmineralien Norwegischer Zinkblendenführender Vorkommen: Oftedal, Ivar. Skrifter uitgitt av Det Norske Videnskaps-Akademi Oslo I. Mat.-Naturv. Klasse Nr 8, 1-103. *Spectrochimica Acta*, **2**, 135. https://doi.org/10.1016/S0371-1951(41)80076-9

[10] Cook, N.J., Ciobanu, C.L., Pring, A., Skinner, W., Shimizu, M., Danyushevsky, L., Saini-Eidukat, B. and Melcher, F. (2009) Trace and Minor Elements in Sphalerite: A LA-ICPMS Study. *Geochimica et Cosmochimica Acta*, **73**, 4761-4791. https://doi.org/10.1016/j.gca.2009.05.045

[11] 毛景文, 杨宗喜, 谢桂青, 袁顺达, 周振华. 关键矿产——国际动向与思考[J]. 矿床地质, 2019, 38(4): 689-698.

[12] 赵汀, 秦鹏珍, 王安建, 王高尚, 李建武, 刘超, 刘毅飞. 镓矿资源需求趋势分析与中国镓产业发展思考[J]. 地球学报, 2017, 38(1): 77-84.

[13] 毛景文, 袁顺达, 谢桂青, 宋世伟, 周琦, 高永宝, 刘翔, 付小方, 曹晶, 曾载淋, 李通国, 樊锡银. 21 世纪以来中国关键金属矿产找矿勘查与研究新进展[J]. 矿床地质, 2019, 38(5): 935-969.

[14] 张伟波, 陈秀法, 陈玉明, 曹艳华, 何学洲, 黄霞, 邓攀. 全球铟矿资源供需现状与我国开发利用建议[J]. 矿产保护与利用, 2019, 39(5): 1-8.

[15] 敦妍冉, 荆海鹏, 洛桑才仁, 张万益, 宋泽峰. 全球镓矿资源分布、供需及消费趋势研究[J]. 矿产保护与利用, 2019, 39(5): 9-15, 25.

[16] 徐净, 李晓峰. 铟矿床时空分布、成矿背景及其成矿过程[J]. 岩石学报, 2018, 34(12): 3611-3626.

[17] 李晓峰, 徐净, 朱艺婷, 吕友虎. 关键矿产资源铟: 主要成矿类型及关键科学问题[J]. 岩石学报, 2019, 35(11): 3292-3302.

[18] Bertelli, M., Williams, P.J., Baker, T., Lisoweic, N. and Boyce, A. (2009) Nature and Origin of Ore-Forming Fluids in the Ravenswood Gold System, North Queensland: Evidence from Fluid Inclusions and Stable Isotopes. *Economic Geology Research Unit*, **1**, 344-346.

[19] Neindorf, L. and Dennis, R. (1989) Ravenswood Gold Mine, an Experience of Rapid Exploration, Development and Production North Queensland Gold 89 Conference.

[20] Mindat.org. Localities: Australia. http://www.mindat.org/loc-186.html, 2020-10-23.

[21] Mindat.org. Localities: Australia. http://www.mindat.org/loc-17051.html, 2020-10-23.

[22] Mindat.org. Localities: Australia. http://www.mindat.org/loc-125689.html, 2020-10-23.

[23] (2006) Australian Company News Bites Stock Report.

[24] (2008) Australian Company News Bites Stock Report.

[25] Ciobanu, C.L., Birch, W.D., Cook, N.J., Pring, A. and Grundler, P.V. (2010) Petrogenetic Significance of Au-Bi-Te-S Associations: The Example of Maldon, Central Victorian Gold Province, Australia. *Lithos*, **116**, 1-17. https://doi.org/10.1016/j.lithos.2009.12.004

[26] Arne, D.C., Bierlein, F.P., Morgan, J.W. and Stein, H.J. (2001) Re-Os Dating of Sulfides Associated with Gold Mineralization in Central Victoria, Australia. *Economic Geology*, **96**, 1455-1459. https://doi.org/10.2113/gsecongeo.96.6.1455

[27] Kucha, H. and Plimer, I.R. (1994) Gold in Organic Matter, Maldon, Victoria, Australia. *Economic Geology*, **94**, 1173-1180. https://doi.org/10.2113/gsecongeo.94.7.1173

[28] (2001) Australian Alps Mining Heritage Conservation & Presentation Strategy.

[29] Mindat.org. Localities: Australia. http://www.mindat.org/loc-65284.html, 2020-10-23.

[30] Solomon, M., Tornos, F., Large, R.R., Badham, J.N.P., Both, R.A. and Zaw, K. (2004) Zn-Pb-Cu Volcanic-Hosted Massive Sulphide Deposits: Criteria for Distinguishing Brine Pool-Type from Black Smoker-Type Sulphide Deposition. *Ore Geology Reviews*, **25**, 259-283. https://doi.org/10.1016/j.oregeorev.2004.01.003

[31] Large, R.R., Allen, R.L., Blake, M.D. and Herrmann, W. (2001) Hydrothermal Alteration and Volatile Element Halos for the Rosebery K Lens Volcanic-Hosted Massive Sulfide Deposit, Western Tasmania. *Economic Geology*, **96**, 1055-1072. https://doi.org/10.2113/gsecongeo.96.5.1055

[32] Pwa, A. and van Moort, J.C. (1999) Geochemical Exploration Using Acid Insoluble Residues of Rocks for Volcanic-Hosted Massive Sulphide Deposits, Rosebery Area, Western Tasmania. *Journal of Geochemical Exploration*, **66**, 55-69. https://doi.org/10.1016/S0375-6742(99)00022-9

[33] Bottrill, R.S., Williams, P.A. and Kemp, N.R. (2006) Crocoite and Associated Minerals from Tasmania. *Australian Journal of Mineralogy*, **12**, 59-90.

[34] Mindat.org. Localities: Australia. http://www.mindat.org/loc-171.html, 2020-10-23.

[35] Barnes, S.J., Gole, M.J. and Hill, R.E.T. (1988) The Agnew Nickel Deposit, Western Australia: Part I. Structure and

Stratigraphy. *Economic Geology*, **83**, 524-536. https://doi.org/10.2113/gsecongeo.83.3.524

[36] Barnes, S.J., Gole, M.J. and Hill, R.E.T. (1988) The Agnew Nickel Deposit, Western Australia; Part II, Sulfide Geochemistry, with Emphasis on the Platinum-Group Elements. *Economic Geology*, **83**, 537-550. https://doi.org/10.2113/gsecongeo.83.3.537

[37] Gole, M.J., Barnes, S.J. and Hill, R.E.T. (1987) The Role of Fluids in the Metamorphism of Komatiites, Agnew Nickel Deposit, Western Australia. *Contributions to Mineralogy and Petrology*, **96**, 151-162. https://doi.org/10.1007/BF00375229

[38] Solomon, M., Gemmell, J.B. and Zaw, K. (2004) Nature and Origin of the Fluids Responsible for Forming the Hellyer Zn-Pb-Cu, Volcanic-Hosted Massive Sulphide Deposit, Tasmania, Using Fluid Inclusions, and Stable and Radiogenic Isotopes. *Ore Geology Reviews*, **25**, 89-124. https://doi.org/10.1016/j.oregeorev.2003.11.001

[39] Mindat.org. Localities: Australia. http://www.mindat.org/loc-48916.html, 2020-10-23.

[40] Bottomer, L.R. (1986) Epithermal Silver-Gold Mineralization in the Drake Area, Northeastern New South Wales. *Journal of the Geological Society of Australia*, **33**, 457-473. https://doi.org/10.1080/08120098608729384

[41] Spry, P.G. and Wonder, J.D. (1989) Manganese-Rich Garnet Rocks Associated with the Broken Hill Lead-Zinc-Silver Deposit, New South Wales, Australia. *Canadian Mineralogist*, **27**, 275-292.

[42] Mindat.org. Localities: Australia. http://www.mindat.org/loc-105886.html, 2020-10-23.

[43] Mindat.org. Localities: Australia. http://www.mindat.org/loc-16479.html, 2020-10-23.

[44] Mindat.org. Localities: Australia. http://www.mindat.org/loc-28499.html, 2020-10-23.

[45] Ashley, P.M., Lottermoser, B.G., Collins, A.J. and Grant, C.D. (2004) Environmental Geochemistry of the Derelict Webbs Consols Mine, New South Wales, Australia. *Environmental Geology*, **46**, 591-604. https://doi.org/10.1007/s00254-004-1063-7

[46] Fernandez, F.G., Both, R.A., Mangas, J. and Arribas, A. (2000) Metallogenesis of Zn-Pb Carbonate-Hosted Mineralization in the Southeastern Region of the Picos de Europa (Central Northern Spain) Province: Geologic, Fluid Inclusion, and Stable Isotope Studies. *Economic Geology*, **95**, 19-40. https://doi.org/10.2113/gsecongeo.95.1.19

[47] Garcia, G.G. and de Baranda, B.S. (1996) The Picos de Europa Lead-zinc Deposits, Spain. *Mineralogical Record*, **27**, 177.

[48] Mindat.org. Localities: Australia. http://www.mindat.org/loc-188.html, 2020-10-23.

[49] Mindat.org. Localities: Australia. http://www.mindat.org/loc-32230.html, 2020-10-23.

[50] Ashley, P.M. and Willott, B.R. (1997) Zinc-Lead Skarn Deposits at Leadville, New South Wales, Australia, and Their Distinction from Volcanic-Hosted Massive Sulphides. *Mineralium Deposita*, **32**, 16-33. https://doi.org/10.1007/s001260050069

[51] Mindat.org. Localities: New Zealand. http://www.mindat.org/loc-15364.html, 2020-10-23.

[52] Karataglis, S.S., McNeilly, T. and Bradshaw, A.D. (1986) Lead and Zinc Tolerance of *Agrostis capillaris* L. and *Festuca rubra* L. across a Mine-Pasture Boundary at Minera, North Wales. *Phyton* (*Austria*), **26**, 65-72.

[53] Mindat.org. Localities: Kosovo. http://www.mindat.org/loc-3052.html, 2020-10-23.

[54] Palinkas, S.S., Palinkas, L.A. and Molnar, F. (2006) Trace-Elements Content of Sphalerite and Associated Minerals in Stari Trg Pb-Zn Deposit, Trepa, Kosovo. *Geochimica et Cosmochimica Acta*, **70**, A468. https://doi.org/10.1016/j.gca.2006.06.1399

[55] Bermanec, V., Avniar, S. and Zebec, V. (1995) Childrenite and Crandallite from the Stari Trg Mine (Trepča), Kosovo: New Data. *Mineralogy & Petrology*, **52**, 197-208. https://doi.org/10.1007/BF01163245

[56] Mindat.org. Localities: Greenland. http://www.mindat.org/loc-30754.html, 2020-10-23.

[57] Sorensen, H., Bailey, J.C. and Rose-Hansen, J. (2011) The Emplacement and Crystallization of the U-Th-REE-Rich Agpaitic and Hyperagpaitic Lujavrites at Kvanefjeld, Límaussaq Alkaline Complex, South Greenland. *Bulletin of the Geological Society of Denmark*, **59**, 69-92. https://doi.org/10.37570/bgsd-2011-59-08

[58] Omori, S. and Mariko, T. (1999) Physicochemical Environment during the Formation of the Mozumi Skarn-Type Pb-Zn-Ag Deposit at the Kamioka Mine, Central Japan: A Thermochemical Study. *Resource Geology*, **49**, 223-232. https://doi.org/10.1111/j.1751-3928.1999.tb00048.x

[59] Mindat.org. Localities: UK. http://www.mindat.org/loc-221672.html, 2020-10-23.

[60] Somerfield, P.J., Gee, J.M. and Warwick, R.M. (1994) Benthic Community Structure in Relation to an Instantaneous Discharge of Waste Water from a Tin Mine. *Marine Pollution Bulletin*, **28**, 363-369. https://doi.org/10.1016/0025-326X(94)90273-9

[61] Hunt, L.E. and Howard, A.G. (1994) Arsenic Speciation and Distribution in the Carnon Estuary Following the Acute

Discharge of Contaminated Water from a Disused Mine. *Marine Pollution Bulletin*, **28**, 33-38. https://doi.org/10.1016/0025-326X(94)90183-X

[62] Mindat.org. Localities: Canada. http://www.mindat.org/loc-514.html, 2020-10-23.

[63] Sherlock, R.L., Lee, J.K.W. and Cousens, B.L. (2004) Geologic and Geochronologic Constraints on the Timing of Mineralization at the Nanisivik Zinc-Lead Mississippi Valley-Type Deposit, Northern Baffin Island, Nunavut, Canada. *Economic Geology*, **99**, 279-293. https://doi.org/10.2113/gsecongeo.99.2.279

[64] McNaughton, K. and Smith, T.E. (1986) A Fluid Inclusion Study of Sphalerite and Dolomite from the Nanisivik Lead-Zinc Deposit, Baffin Island, Northwest Territories, Canada. *Economic Geology*, **81**, 713-720. https://doi.org/10.2113/gsecongeo.81.3.713

[65] Arne, D.C. and Kissin, S.A. (1989) The Significance of "Diagenetic Crystallization Rhythmites" at the Nanisivik Pb-Zn-Ag Deposit, Baffin Island, Canada. *Mineralium Deposita*, **24**, 230-232. https://doi.org/10.1007/BF00206447

[66] Ghazban, F., Schwarcz, H.P. and Ford, D.C. (1990) Carbon and Sulfur Isotope Evidence for *in Situ* Reduction of Sulfate, Nanisivik Lead-Zinc Deposits, Northwest Territories, Baffin Island, Canada. *Economic Geology*, **85**, 360-375. https://doi.org/10.2113/gsecongeo.85.2.360

[67] Arne, D.C., Curtis, L.W. and Kissin, S.A. (1991) Internal Zonation in a Carbonate-Hosted Zn-Pb-Ag Deposit. Nanisivik, Barfin Island, Canada. *Economic Geology*, **86**, 699-717. https://doi.org/10.2113/gsecongeo.86.4.699

[68] Mindat.org. Localities: Ireland. http://www.mindat.org/loc-4495.html, 2020-10-23.

[69] Schneider, J., Quadt, A.V., Wilkinson, J.J. and Boyce, A.J. (2007) Age of the Silvermines Irish-Type Zn-Pb Deposit from Direct Rb-Sr Dating of Sphalerite. *Proceedings of the* 9*th Biennial SGA Meeting*, Dublin, 20-23 August 2007, 373-376.

[70] Reed, C.P. and Wallace, M.W. (2004) Zn-Pb Mineralisation in the Silvermines District, Ireland: A Product of Burial Diagenesis. *Mineralium Deposita*, **39**, 87-102. https://doi.org/10.1007/s00126-003-0384-x

[71] Kucha, H. (1989) Macrotextures, Microtextures, and Carbonate-Sulfide Relationships in Stratiform, Carbonate-Hosted Zn-Pb Orebodies of Silvermines, Ireland. *Mineralium Deposita*, **24**, 48-55. https://doi.org/10.1007/BF00206723

[72] Samson, I.M. and Russell, M.J. (1987) Genesis of the Silvermines Zinc-Lead-Barite Deposit, Ireland; Fluid Inclusion and Stable Isotope Evidence. *Economic Geology*, **82**, 371-394. https://doi.org/10.2113/gsecongeo.82.2.371

[73] Taylor, S. (1984) Structural and Paleotopographic Controls of Lead-Zinc Mineralization in the Silvermines Orebodies, Republic of Ireland. *Economic Geology*, **79**, 529-548. https://doi.org/10.2113/gsecongeo.79.3.529

[74] Mindat.org. Localities: Australia. http://www.mindat.org/loc-121096.html, 2020-10-23.

[75] Symons, D.T.A. and Arne, D.C. (2003) Paleomagnetic Dating of Mineralization in the Kapok MVT Deposit, Lennard Shelf, Western Australia. *Journal of Geochemical Exploration*, **78-79**, 267-272. https://doi.org/10.1016/S0375-6742(03)00022-0

[76] Eggins, S.M., Woodhead, J.D., Kinsley, L.P.J., Mortimer, G.E. and Handler, M.R. (1997) A Simple Method for the Precise Determination of ≥ 40 Trace Elements in Geological Samples by ICPMS Using Enriched Isotope Internal Standardisation. *Chemical Geology*, **134**, 311-326. https://doi.org/10.1016/S0009-2541(96)00100-3

[77] Lin, Y., Cook, N.J., Ciobanu, C.L., Liu, Y.P., Liu, T.G., Gao, W., Yang, Y.L. and Danyushevskiy, L. (2011) Trace and Minor Elements in Sphalerite from Base Metal Deposits in South China: A LA-ICPMS Study. *Ore Geology Reviews*, **39**, 188-217. https://doi.org/10.1016/j.oregeorev.2011.03.001

[78] Seifert, T. and Sandmann, D. (2006) Mineralogy and Geochemistry of Indium-Bearing Polymetallic Vein-Type Deposits: Implications for Host Minerals from the Freiberg District, Eastern Erzgebirge, Germany. *Ore Geology Reviews*, **28**, 1-31. https://doi.org/10.1016/j.oregeorev.2005.04.005

[79] Sclzaefer, M.O. and Gutzmer, J. (2004) Mineral Chemistry of Sphalerite and Galena from Pb-Zn Mineralization Hosted by the Transvaal Supergroup in Griqualand West, South Africa. *South African Journal of Geology*, **107**, 341-354. https://doi.org/10.2113/107.3.341

附 表

Table A1. Sample information collected in the literatures
表 A1. 文献中收集的样品信息

序号	样品编号 (分析数量)	实验室	分析方法 (测试样品方式)	成因类型	工业类型	参考文献
1	Baia de Aries BdA (6)	CODES (University of Tasmania)	LA-ICPMS (polished mounts)	Hydrothermal (Epithermal)	Zn-Pb	[10]
2	Hanes H-1962 (8)	CODES (University of Tasmania)	LA-ICPMS (polished mounts)	Hydrothermal (Epithermal)	Au	[10]
3	Larga L-82 (8)	CODES (University of Tasmania)	LA-ICPMS (polished mounts)	Hydrothermal (Epithermal)	Au	[10]
4	Rosia Montana CRC-7 (10)	CODES (University of Tasmania)	LA-ICPMS (polished mounts)	Hydrothermal (Epithermal)	Au	[10]
5	Rosia Montana RM-21 (10)	CODES (University of Tasmania)	LA-ICPMS (polished mounts)	Hydrothermal (Epithermal)	Au	[10]
6	Magura Mag-8 (8)a	CODES (University of Tasmania)	LA-ICPMS (polished mounts)	Hydrothermal (Epithermal)	Au	[10]
7	Sacarimb Sac 7.3 (6)	CODES (University of Tasmania)	LA-ICPMS (polished mounts)	Hydrothermal (Epithermal)	Au	[10]
8	Sacarimb Sac 7.7 (5)	CODES (University of Tasmania)	LA-ICPMS (polished mounts)	Hydrothermal (Epithermal)	Au	[10]
9	Toroiaga Tga-1 (6)	CODES (University of Tasmania)	LA-ICPMS (polished mounts)	Hydrothermal (Epithermal)	Au	[10]
10	In-1 low-In (3)	CODES (University of Tasmania)	LA-ICPMS (polished mounts)	Hydrothermal (Epithermal)	Zn-Pb-Cu	[10]
11	In-1 high-In (7)	CODES (University of Tasmania)	LA-ICPMS (polished mounts)	Hydrothermal (Epithermal)	Zn-Pb-Cu	[10]
12	In-1 high-Sn (8)	CODES (University of Tasmania)	LA-ICPMS (polished mounts)	Hydrothermal (Epithermal)	Zn-Pb-Cu	[10]
13	In-2 (4)	CODES (University of Tasmania)	LA-ICPMS (polished mounts)	Hydrothermal (Epithermal)	Zn-Pb-Cu	[10]
14	Majdanpek MD-20 (8)	CODES (University of Tasmania)	LA-ICPMS (polished mounts)	Skarn	Zn-Pb	[10]
15	OdF P43 low-Fe (9)	CODES (University of Tasmania)	LA-ICPMS (polished mounts)	Skarn	Zn	[10]
16	OdF 3375 (6)	CODES (University of Tasmania)	LA-ICPMS (polished mounts)	Skarn	Zn	[10]
17	OdF 3910b (8)	CODES (University of Tasmania)	LA-ICPMS (polished mounts)	Skarn	Zn	[10]
18	OdF 54G (6)	CODES (University of Tasmania)	LA-ICPMS (polished mounts)	Skarn	Zn	[10]
19	OdF St1 (6)	CODES (University of Tasmania)	LA-ICPMS (polished mounts)	Skarn	Zn	[10]
20	BB19CB (6)	CODES (University of Tasmania)	LA-ICPMS (polished mounts)	Skarn	Cu	[10]

Continued

21	BB16C (6)	CODES (University of Tasmania)	LA-ICPMS (polished mounts)	Skarn	Zn-Pb	[10]
22	BB6 (8)	CODES (University of Tasmania)	LA-ICPMS (polished mounts)	Skarn	Zn-Pb	[10]
23	BB23 (10)	CODES (University of Tasmania)	LA-ICPMS (polished mounts)	Skarn	Zn-Pb	[10]
24	VS 1b (6)	CODES (University of Tasmania)	LA-ICPMS (polished mounts)	Skarn	Zn-Pb	[10]
25	Bs7a (11)	CODES (University of Tasmania)	LA-ICPMS (polished mounts)	Skarn	Zn-Pb	[10]
26	Bs7g (10)	CODES (University of Tasmania)	LA-ICPMS (polished mounts)	Skarn	Zn-Pb	[10]
27	Kamioka Kam-1 (8)	CODES (University of Tasmania)	LA-ICPMS (polished mounts)	Skarn	Zn-Pb	[10]
28	Lefevre (CLY) L-12 (8)	CODES (University of Tasmania)	LA-ICPMS (polished mounts)	Skarn	Zn-Pb	[10]
29	Konnerudkollen Ko99.2 (5)	CODES (University of Tasmania)	LA-ICPMS (polished mounts)	Skarn	Zn-Pb	[10]
30	TM low-Fe (10)	CODES (University of Tasmania)	LA-ICPMS (polished mounts)	Stratabound	Zn-Pb	[10]
31	TM-high-Fe (12)	CODES (University of Tasmania)	LA-ICPMS (polished mounts)	Stratabound	Zn-Pb	[10]
32	Sinkholmen Znh1 (8)	CODES (University of Tasmania)	LA-ICPMS (polished mounts)	Stratabound	Zn-Pb	[10]
33	Kapp Mineral KMi5 (10)	CODES (University of Tasmania)	LA-ICPMS (polished mounts)	Stratabound	Zn-Pb	[10]
34	Hitra Hit-1 (8)	CODES (University of Tasmania)	LA-ICPMS (polished mounts)	Stratabound	Zn-Pb	[10]
35	Vorta DMV (8)	CODES (University of Tasmania)	LA-ICPMS (polished mounts)	VMS	Au-Ag	[10]
36	Eskay Creek P5 (12)	CODES (University of Tasmania)	LA-ICPMS (polished mounts)	VMS	Cu	[10]
37	Sauda Sa-1 (10)	CODES (University of Tasmania)	LA-ICPMS (polished mounts)	VMS	Zn	[10]
38	Zinkgruvan Zn99.2 (5)	CODES (University of Tasmania)	LA-ICPMS (polished mounts)	VMS	Zn-Pb-Ag	[10]
39	Kaveltorp Kv99.1 (7)	CODES (University of Tasmania)	LA-ICPMS (polished mounts)	VMS	Cu-Zn-Pb	[10]
40	Marketorp Ma99.4 (8)	CODES (University of Tasmania)	LA-ICPMS (polished mounts)	VMS	Cu-Zn-Pb	[10]
41	3115X-37	Geological Survey of Canada	Electron Microprobe (polished thin sections)	—	Sn	[8]
42	5497-3-28	Geological Survey of Canada	Electron Microprobe (polished thin sections)	—	Sn	[8]
43	8381-8	Geological Survey of Canada	Electron Microprobe (polished thin sections)	—	Sn	[8]

Continued

44	10428D-1-5	Geological Survey of Canada	Electron Microprobe (polished thin sections)	—	Sn	[8]
45	14488-117	Geological Survey of Canada	Electron Microprobe (polished thin sections)	—	Sn	[8]
46	222(202)	TU Bergakademie Freiberg	Electron Microprobe (polished sections)	Hydrothermal	Ag	[78]
47	50437-1A(5)	TU Bergakademie Freiberg	Electron Microprobe (polished sections)	Hydrothermal	Ag	[78]
48	50437-1B(25)	TU Bergakademie Freiberg	Electron Microprobe (polished sections)	Hydrothermal	Ag	[78]
49	Zinnw1-5(19)	TU Bergakademie Freiberg	Electron Microprobe (polished sections)	Hydrothermal	Sn	[78]
50	Sample 1A	Finnigan MAT, Bremen, Germany	LA-ICP-SFMS (sample fragments)	—	Zn	[1]
51	Sample 1B	Finnigan MAT, Bremen, Germany	SN-ICP-SFMS (grains)	—	Zn	[1]
52	Sample 2A	Finnigan MAT, Bremen, Germany	LA-ICP-SFMS (sample fragments)	—	Zn	[1]
53	Sample 2B	Finnigan MAT, Bremen, Germany	SN-ICP-SFMS (grains)	—	Zn	[1]
54	Sample 3A	Finnigan MAT, Bremen, Germany	LA-ICP-SFMS (sample fragments)	—	Zn	[1]
55	Sample 3B	Finnigan MAT, Bremen, Germany	SN-ICP-SFMS (grains)	—	Zn	[1]
56	Sample 4A	Finnigan MAT, Bremen, Germany	LA-ICP-SFMS (sample fragments)	—	Zn	[1]
57	Sample 4B	Finnigan MAT, Bremen, Germany	SN-ICP-SFMS (grains)	—	Zn	[1]
58	Sample 5A	Finnigan MAT, Bremen, Germany	LA-ICP-SFMS (sample fragments)	—	Zn	[1]
59	Sample 5B	Finnigan MAT, Bremen, Germany	SN-ICP-SFMS (grains)	—	Zn	[1]
60	1	Manchester	Electron Microprobe (polished sections)	Skarn	Cu-Au	[3]
61	1164	Manchester	Electron Microprobe (polished sections)	Hydrothermal	Pb-Zn	[3]
62	1165bis	Manchester	Electron Microprobe (polished sections)	Hydrothermal	Pb-Zn	[3]
63	1168	Manchester	Electron Microprobe (polished sections)	Hydrothermal	Pb-Zn	[3]
64	1188	Manchester	Electron Microprobe (polished sections)	Hydrothermal	Pb-Zn	[3]
65	1189	Manchester	Electron Microprobe (polished sections)	Hydrothermal	Pb-Zn	[3]
66	1206	Manchester	Electron Microprobe (polished sections)	Skarn	Pb-Zn-Cu	[3]

Continued

67	1210	Manchester	Electron Microprobe (polished sections)	Skarn	Pb-Zn-Cu	[3]
68	1211	Manchester	Electron Microprobe (polished sections)	Skarn	Pb-Zn-Cu	[3]
69	1212	Manchester	Electron Microprobe (polished sections)	Hydrothermal (Epithermal)	Pb-Zn-Cu	[3]
70	1215	Manchester	Electron Microprobe (polished sections)	Hydrothermal (Epithermal)	Pb-Zn-Cu	[3]
71	1227	Manchester	Electron Microprobe (polished sections)	Hydrothermal (Epithermal)	Pb-Zn-Cu	[3]
72	1257	Manchester	Electron Microprobe (polished sections)	Hydrothermal (Epithermal)	Pb-Zn-Cu	[3]
73	1276	Manchester	Electron Microprobe (polished sections)	Skarn	Pb-Zn	[3]
74	1293	Manchester	Electron Microprobe (polished sections)	Hydrothermal	Pb-Zn	[3]
75	1303	Manchester	Electron Microprobe (polished sections)	Hydrothermal	Pb-Zn	[3]
76	47975	Manchester	Electron Microprobe (polished sections)	MVT	Zn-Pb	[3]
77	22551	Manchester	Electron Microprobe (polished sections)	VMS	—	[3]
78	HTP-27	CODES (University of Tasmania)	LA-ICPMS (polished mounts)	Skarn	Zn-Pb	[77]
79	HTP-174	CODES (University of Tasmania)	LA-ICPMS (polished mounts)	Skarn	Zn-Pb	[77]
80	HTP-163	CODES (University of Tasmania)	LA-ICPMS (polished mounts)	Skarn	Zn-Pb	[77]
81	LZY-47	CODES (University of Tasmania)	LA-ICPMS (polished mounts)	Skarn	Zn-Pb	[77]
82	LZY-29	CODES (University of Tasmania)	LA-ICPMS (polished mounts)	Skarn	Zn-Pb	[77]
83	LZY-61	CODES (University of Tasmania)	LA-ICPMS (polished mounts)	Skarn	Zn-Pb	[77]
84	DBS-1	CODES (University of Tasmania)	LA-ICPMS (polished mounts)	SEDEX	Zn-Pb	[77]
85	DBS-2	CODES (University of Tasmania)	LA-ICPMS (polished mounts)	SEDEX	Zn-Pb	[77]
86	DBS-6	CODES (University of Tasmania)	LA-ICPMS (polished mounts)	SEDEX	Zn-Pb	[77]
87	BNC-3	CODES (University of Tasmania)	LA-ICPMS (polished mounts)	SEDEX	Sn	[77]
88	BNC-10	CODES (University of Tasmania)	LA-ICPMS (polished mounts)	SEDEX	Sn	[77]
89	LC-9	CODES (University of Tasmania)	LA-ICPMS (polished mounts)	VMS	Zn-Pb	[77]

Continued

90	LC-19	CODES (University of Tasmania)	LA-ICPMS (polished mounts)	VMS	Zn-Pb	[77]
91	LC-18	CODES (University of Tasmania)	LA-ICPMS (polished mounts)	VMS	Zn-Pb	[77]
92	HZF-1086	CODES (University of Tasmania)	LA-ICPMS (polished mounts)	MVT	Zn-Pb	[77]
93	HZF-1062	CODES (University of Tasmania)	LA-ICPMS (polished mounts)	MVT	Zn-Pb	[77]
94	HZF-1065	CODES (University of Tasmania)	LA-ICPMS (polished mounts)	MVT	Zn-Pb	[77]
95	B-10	CODES (University of Tasmania)	LA-ICPMS (polished mounts)	MVT	Zn-Pb	[77]
96	B-6	CODES (University of Tasmania)	LA-ICPMS (polished mounts)	MVT	Zn-Pb	[77]
97	H-22	CODES (University of Tasmania)	LA-ICPMS (polished mounts)	MVT	Zn-Pb	[77]
98	M-1	CODES (University of Tasmania)	LA-ICPMS (polished mounts)	MVT	Zn-Pb	[77]
99	M-11	CODES (University of Tasmania)	LA-ICPMS (polished mounts)	MVT	Zn-Pb	[77]
100	M	CODES (University of Tasmania)	LA-ICPMS (polished mounts)	*Sandstone-hosted*	Zn-Pb	[77]
101	Jind-150	CODES (University of Tasmania)	LA-ICPMS (polished mounts)	*Sandstone-hosted*	Zn-Pb	[77]
102	Jind-148	CODES (University of Tasmania)	LA-ICPMS (polished mounts)	*Sandstone-hosted*	Zn-Pb	[77]
103	Jind-155-26	CODES (University of Tasmania)	LA-ICPMS (polished mounts)	*Sandstone-hosted*	Zn-Pb	[77]
104	BP368-263.9	The Rand Afrikaans University	ICPMS (grain mounts)	MVT	Pb-Zn	[79]
105	CR-5R	The Rand Afrikaans University	ICPMS (grain mounts)	MVT	Pb-Zn	[79]
106	CR-24.8R	The Rand Afrikaans University	ICPMS (grain mounts)	MVT	Pb-Zn	[79]
107	S-274	The Rand Afrikaans University	ICPMS (grain mounts)	MVT	Pb-Zn	[79]
108	B8-1	The Rand Afrikaans University	ICPMS (grain mounts)	MVT	Pb-Zn	[79]
109	Ba-5	The Rand Afrikaans University	ICPMS (grain mounts)	MVT	Pb-Zn	[79]
110	B8-3	The Rand Afrikaans University	ICPMS (grain mounts)	MVT	Pb-Zn	[79]
111	GAP-5	The Rand Afrikaans University	ICPMS (grain mounts)	MVT	Pb-Zn	[79]
112	GBP-2	The Rand Afrikaans University	ICPMS (grain mounts)	MVT	Pb-Zn	[79]

Continued

113	GBP-1	The Rand Afrikaans University	ICPMS (grain mounts)	MVT	Pb-Zn	[79]
114	GAP-4	The Rand Afrikaans University	ICPMS (grain mounts)	MVT	Pb-Zn	[79]
115	EH16-106.7	The Rand Afrikaans University	ICPMS (grain mounts)	MVT	Pb-Zn	[79]
116	P1-8	The Rand Afrikaans University	ICPMS (grain mounts)	MVT	Pb-Zn	[79]
117	P91-45.6	The Rand Afrikaans University	ICPMS (grain mounts)	MVT	Pb-Zn	[79]
118	P1-107.4	The Rand Afrikaans University	ICPMS (grain mounts)	MVT	Pb-Zn	[79]
119	P1-101.7	The Rand Afrikaans University	ICPMS (grain mounts)	MVT	Pb-Zn	[79]